GRADUATE SCHOOL OF OCEANOGRAPHY
UNIVERSITY OF RHODE ISLAND
NARRAGANSETT, RHODE ISLAND

An intercomparison of four models of Current Meter in high current conditions in Drake Passage

GSO Technical Report 12-04

by
Maureen A. Kennelly, D. Randolph Watts, Karen L. Tracey,
and Kathleen A. Donohue

November 7, 2012

ABSTRACT - DRAFT

Seven current meters representing four models were placed for an 11 month deployment on a stiffly buoyed mooring to intercompare their velocity measurements: two VMCMs, two Aanderaa RCM11s, two Aanderaa SEAGUARDSs, and a Nortek Aquadopp. The current meters were placed 6 m apart from each other at about 4000 m depth in an area of Drake Passage expected to have strong near-bottom currents, that were nearly independent of depth. Two high-current events occurred in bursts of semi-diurnal pulses lasting several days, one with peak speeds up to 67 cm s^{-1} and the other above 35 cm s^{-1}. The current speed measurements all agreed within about 5% when vector-averaged over simultaneous time intervals: the full time interval (198 days) when all instruments were working, and the two high-speed events lasting 21 days and 7 days. The VMCMs, chosen as the reference measurements, were found to measure the median of the mean-current magnitudes. The RCM11 and SEAGUARD current speeds had a nearly 1:1 relationship with the median. They agreed within 2% at higher speeds (35–70 cm s^{-1}), whereas in lower speed ranges (0–35 cm s^{-1}) the vector-averaged speeds for the RCM11s and SEAGUARDS were, respectively, 4–5% lower and 3–5% higher than the median. The Aquadopp current speeds were about 7% higher than the VMCMs over the range (0–40 cm s^{-1}) encountered through their shorter common time period.

Contents

List of Figures

List of Tables

1 Introduction

We report here on results of an opportunity to compare current measurements from three different-model acoustic Doppler single-height current meters and the vector measuring current meter (VMCM) [*Weller and Davis*, 1980], which we judged to be standardly characterized by preceding tow-tank tests. This new comparison was conducted on a moored deployment, because for acoustic Doppler current sensors, a calibration test in a tow-tank is not suitable due to acoustic reflections off the side walls. For reasons summarized below, our chief aim was to obtain comparisons at speeds in excess of 35 cm s^{-1}, and we are pleased to report on records with observed current speeds spanning up to 70 cm s^{-1} (67 cm s^{-1}) uncorrected (corrected).

A broad review of modern current measuring techniques has been given in *Dickey et al.* [1998]. Comparisons between the VMCM and other acoustic Doppler current measurements have been performed utilizing a surface mooring known as the Bermuda Testbed Mooring, as summarized by *Gilboy et al.* [2000].

Hogg and Frye [2007] conducted extensive tests between the Aanderaa RCM11 acoustic Doppler current sensor, and conventional vector averaging and vector measuring current meters (VACM and VMCM) and found that the RCM11 recorded consistently lower speeds than the conventional current meters. Their tests were limited to conditions with current speeds less than about 35 cm s^{-1}. Within that low-speed range, personal communications with Hogg suggested that a speed-correction factor of 1.1 should be applied to the RCM11 speeds.

Weller (personal communication) tested RCM11s against VMCMs off the northern coast of Chile beneath an air-sea flux buoy in the upper 300 m of the water column. Maximum speeds were below 40 cm s^{-1}, and in contrast to the preceding case, the speed-correction factor did not differ significantly from 1.0. Weller's results suggested that the RCM11 tilt sensor should be turned off, because it was on a surface mooring with substantial mooring motions (accelerations) that may affect a tilt sensor. In addition the upper water column may have had significant vertical shear. So the test gave evidence that speeds agreed between VMCMs and RCM11s (without tilt compensation), but it was inconclusive regarding high current regimes.

Drozdowski et al. [2010] at BIO-DFO-Halifax intercompared five current meter models (SEAGUARD, Teledyne RDI Doppler Volume Sampler (DVS), RCM8, RCM11 and 300 kHz Teledyne RDI ADCP) on a shallow mooring deployed for three weeks on the Scotian Shelf in 2008. The current speeds observed were less than 40 cm s^{-1}. BIO subsequently deployed the same instruments for a year in water deeper than 1500 m also on the Scotian Shelf, but

again the speeds were less than 26 cm s^{-1} [*Drozdowski and Greenan*, 2012].

Houk and Johns (unpublished manuscript) compared data from three different models of single-point acoustic Doppler current meters (a Nortek Deep-Water Aquadopp, a Teledyne RDI DVS and an Aanderaa SEAGUARD) from an 18-month deployment (December 2009 - April 2011). They found that differences between measurements were close to expected uncertainties, but also found a slight bias in speed and direction in the Aquadopp compared to the DVS and SEAGUARD. The bias increased slightly with increasing current speed.

The results of several recent intercomparison studies with SEAGUARDS are summarized in *Victoria* [2011].

During the first-year (2007–2008) deployment in cDrake (http://www.cDrake.org), RCM11 current meter sensors located 50 m above the seafloor on CPIES observed several high-speed current events [*Chereskin et al.*, 2009]. Events with peak speeds of 60–70 cm s^{-1} typically lasted a week or more at a suite of sites within the Local Dynamics Array, which had been centered upon an eddy kinetic energy hot-spot at the sea surface. The question naturally arose whether a speed-correction factor should be applied to the RCM11 at these speeds.

We received NSF funding for an approximately one-year deployment of a short near-bottom mooring in the cDrake Local Dynamics Array, that would compare two RCM11s, two VMCMs, two Aanderaa ZPulse RCMs on SEAGUARD data loggers, and a Nortek Deep-Water Aquadopp. These current meters were placed as close together as operationally practical with nominal 6 m separation; their heights ranged 98 m to 136 m above the seafloor to avoid the benthic boundary layer. A site was chosen where weak stratification indicated vertical shear should be negligible. Hence they should all observe the same current. The logistics were relatively simple because we already had cruises and personnel scheduled for cDrake operations. Other advantages of conducting this comparison in the deep ocean were that a short deep mooring could be designed to reduce tilt and mooring motion for these expected high currents, and it would avoid near-surface hazards such as biofouling, ice, and fishing/trawling activities.

2 Mooring Design

Our mooring design used established procedures and hardware components, plus specialized low-drag buoyancy described below (Figure 1). We sought a balance between

1. placing instruments more than 3 m apart to avoid spurious side-lobe acoustic reflections off mooring components and with at least 5 m wire between them to enable individual handling during launch and recovery, versus

2. achieving minimal mooring motion and tilt in strong currents by using short wire lengths and low-drag components.

Seven current meters representing four different models were on the mooring: two Aanderaa RCM11s, two Aanderaa SEAGUARD ZPulse RCMs, two VMCMs and one Nortek Deep-Water Aquadopp (Figure 1). The RCM11s were located at levels 1 (no tilt correction) and 4 (tilt correction), the VMCMs at levels 2 and 6, the SEAGUARDs at levels 3 (tilt correction) and 5 (no tilt correction), and the Aquadopp was at level 7 (Table 1). All current meters were nominally separated by 6 m, all maintained close together to produce measurements of nearly the same currents.

All buoyancy was at the top of the mooring, starting with three 17-inch glass spheres on a radio-flasher relocation aid. Next, twelve glass flotation spheres were housed in six OpenSeas Instrumentation, Inc., shells, called Streamlined Underwater Buoyancy System (SUBS). Each SUBS shell holds two standard 17-inch glass spheres. For equivalent buoyancy, the SUBS produce roughly one-quarter the drag of customary chained clusters of glass spheres in hard hats. All main lengths of mooring line were 3/16 inch jacketed wire rope. At the bottom of the mooring were dual ORE 8242 acoustic releases and a 2000 lb cast iron anchor.

The RCM11s, VMCMs, and Aquadopp were provided and prepared by the Woods Hole Oceanographic Institution. The SEAGUARDs were loaned and prepared by Aanderaa Data Instruments Incorporated. Final checkouts and startup were performed aboard ship prior to launch.

The start and end times aboard ship for the current meters are listed in Table 1. The sampling interval for the VMCMs was set to one minute, all other current meters were set to 30 minutes. A summary of current meter specifications is given in Table 2.

The following subsections provide current meter model specific and deployment details.

2.1 Aanderaa RCM11

The RCM11s were configured to record four channels: channel 1 is a reference, while channels two through four are respectively current speed, current direction and temperature. Currents were measured in spread mode: during the 30-minute measurement interval, the instrument transmitted 600 evenly distributed pings. u and v are averaged over the sampling interval and from the resulting averages, speed and direction are calculated. The time stamp occurs at the end of the measurement interval.

Alkaline batteries (15 Ah battery power) were used in the RCM11s. Upon return, we learned that the high ping rate and 30-minute sampling interval selected should have resulted in only 248 days (8.3 months of the 11 month deployment) of data according to the manufacturer's specifications. In fact, the RCM11s recorded for about a month and a half longer than the battery calculation predicted. If a 30 Ah lithium battery would have been used the instruments would have sampled for the entire deployment period.

2.2 VMCM

The VMCM [*Weller and Davis*, 1980] has two orthogonal cosine-response impeller sensors that measure the components of horizontal current velocity along the rotation axes of each impeller. The orientation of the instrument chassis relative to magnetic north is determined by a flux-gate compass. A lubber line and a pin in the rotor/impeller assembly aligns the impeller geometry to the chassis and compass. East and north components of velocity are computed nearly continuously with each 1/4 turn of the impeller; these are averaged and then stored on flash memory cards. An averaging interval of one minute was used for data recorded in this study.

Following are additional notes from Bob Weller and his engineers.

1. Speed Calibration:

The speed calibration is 2.67 propeller revolutions per meter of flow. With 4 counts per revolution, 1 count = 10 cm of flow.

2. Stall speeds:

There are magentodiodes inside the rotor hubs; each diode has a ferritic flux concentrator so there is magnetic attraction between the magnets in the encoder on the impeller shaft and the magnetodiodes. There is a magnetic force that preloads the ball bearings and increases threshold speed for flow parallel to rotor axles to ≈ 2.5 cm s^{-1}. With cosine angular response, if the flow is off axle and the prop is not moving, break-free occurs at a higher speed. This sometimes has been observed on deep quiet subsurface moorings.

3. Rotor-blocking Diagnostics:

At each [quarter-turn] count, the cosine and sine are computed and stored; the compass is updated [at a more rapid rate for that purpose]. The impellers up-count and down-count, so there is a sign associated with counts R1 and R2. At end of 1 minute the accumulated vector contributions from rotor 1 and rotor 2 give a 1-min vector average u and v. The number of quarter-revolutions of each impeller, R1 and R2 counts, also get recorded as diagnostics. (If one rotor is stopped due to fishing line, a u and a v would still have been recorded from one rotor, but you would not have known they were wrong if you did not also record rotor count totals for the minute.)

4. Tilt compensation:

With the original compass, tilt was not measured. With newer models, tilt_x and tilt_y are measured and recorded as the last reading each minute (Allsup, personal communication). Nevertheless, lateral acceleration may affect tilts, so Weller never pressed for firmware to do tilt correction.

The method we used to apply a tilt correction is described in Section 4, where we show that tilt correction brought the speed records from all instruments into substantially improved agreement.

The TCM2-20 is spec'd to 20 degrees tilt, but it performs up to 22-to-26 degrees tilt, and the maximum logged value by the VMCM firmware is 25.5 degrees. The tilt_x maximum for VMCM 002 reached 25.5, so at first we were concerned that the tilt may have exceeded that value, and might have been chopped to the maximum logged value of 25.5. The total tilt plot (see Figure 5) of the SEAGUARD neighboring above it looks consistent, indicating that if chopping occurred for VMCM 002, it was not appreciable. The Aquadopp that neighbored below it had quit before that maximum-tilt event.

2.3 Aanderaa SEAGUARD RCM

The SEAGUARD dataloggers were equipped with ZPulse multi-frequency Doppler current sensors (DCS), plus pressure, conductivity, and oxygen sensors (Table 3). Each of those sensors has its own temperature measurement. The SEAGUARDs were powered by lithium batteries.

The DCS, pressure, conductivity, and oxygen sensors were verified aboard ship prior to launch. The 150 ohm test-resistor was looped through the conductivity sensor during the first sample for both instruments, and the conductivity registered correctly about 31.

SeaGuard Studio version 1.5 software was used. The system-configuration wizard confirmed the following settings for both instruments: number of pings is 300 (equivalent to 600, accounting for the two frequencies transmitted in each ping). Both SEAGUARDs were

configured in 'burst mode' (300 pings in the last 60 seconds of the recording interval). The time stamp occurs at the end of the measurement interval. The recorded currents are the vector average of each burst measurement.

Sound speed is 1500 m s^{-1}. Start distance is 0.5 m, and cell size is 1.5 m; hence the acceptance window for reflections extends from 0.5 m to 2.0 m. Transducer activation was set to 1-and-3 for the x-axis, 2-and-4 for the y-axis, and forward ping active was selected, meaning that positive Doppler shifts were analyzed from unperturbed water approaching the sensor. Tilt correction was enabled for the upper SEAGUARD (SN 137), but 'off' for the lower one (SN 136).

2.4 Nortek Aquadopp

The Aquadopp was mounted pointing downward on this mooring. Tilt is automatically compensated in the Aquadopp software. The maximum sampling rate is 23 Hz. For this deployment, the measurement load was set to 4% (0.92 Hz) and the burst averaging interval was set to 120 seconds. This yields 110 samples (0.92 Hz * 120 seconds) in a 2-minute average. The time stamp occurs at the start of the burst-averaging interval. The measurement interval for burst-sampling was 1800 s (30 min). The compass update rate is two seconds. The recorded currents are the vector average of each burst measurement. Current is compensated for a variable speed of sound, which is calculated from measured temperature and a constant salinity of 35 ppt. Current speed, calculated in post-processing by the Aquadopp software (version 1.31 used here), differs slightly from the vector-averaged (u, v) speed. Deepwater velocity scaling was not applied to the speed value. Newer versions of the software ($>$ version 1.36) correct for this difference.

Alkaline batteries were installed in the Aquadopp. Using the Nortek battery budget, the Aquadopp should have sampled for 13 months. However, it only recorded for nine months. The batteries in the Aquadopp were depleted, although battery consumption estimates indicated that the current meter should have sampled for the full deployment period, with adequate reserve energy. We surmise that the batteries may have been subjected to high temperatures during shipment from Rhode Island by surface through Los Angeles (in August), and subsequently by container to Punta Arenas, Chile.

2.5 Deployment

The mooring, designated M04, was deployed on 24 November 2009 at 56.55°S, 62.15°W in the cDrake Local Dynamics Array (Figure 2). The mooring took 45 minutes to reach the seafloor, at which time we communicated with the two releases and confirmed that the

mooring stood upright.

After an 11-month deployment, recovery began on 28 October 2010 when the mooring was released at 1620 UTC. The mooring rise rate was about 32 m min^{-1}, which was much slower than expected. Upon recovery it was discovered that two glass balls had broken.

Two of the SUBS buoys had one broken glass ball each (two broken balls total). Both broken balls were in the front ends of the buoys. The glass looked broken by impact rather than imploded at high pressure. A high-pressure implosion would have ripped open the plastic shell of the SUBS. We do not think the glass balls were broken in the course of the launch, because the operations proceeded without apparent impacts. So we infer that the glass balls were cracked prior to deployment, during shipping and handling in 2009.

Upon recovery we discovered that the radio/flasher battery was dead. We think that its battery was drained because the mooring (with partially lost buoyancy) tilted enough to trigger its mercury tilt-switch and repeatedly reactivated the radio/flasher ball during the strong eddy events throughout the year. A mercury tilt-switch is not adequate for future deployments at high-current sites.

The current meters and releases looked in great condition upon recovery except for aluminum corrosion around the top of the VMCM housings, not affecting measurements. The SUBS black plastic 'vanes' showed significant damage; many of the vanes were broken or chipped.

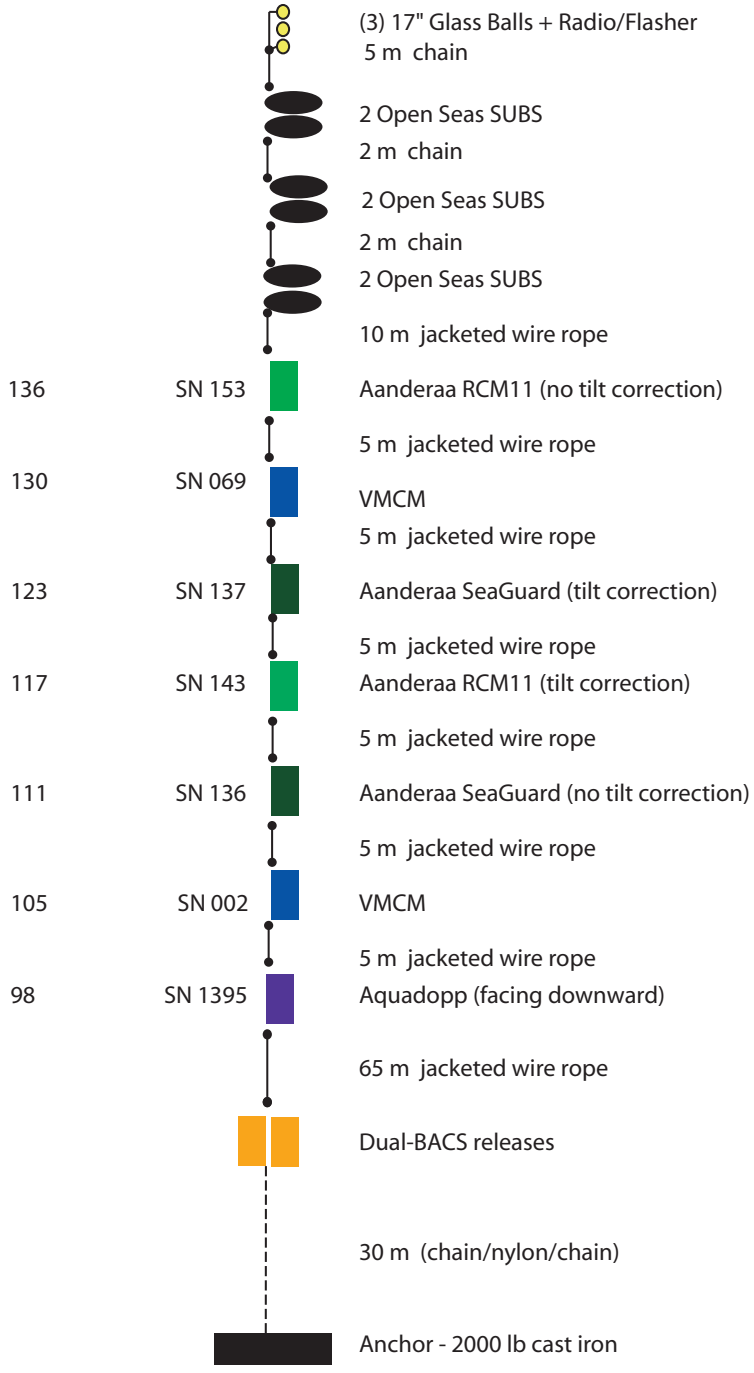

Figure 1: Mooring schematic. Numbers to the left of the current meter serial numbers are heights above the ocean bottom (m).

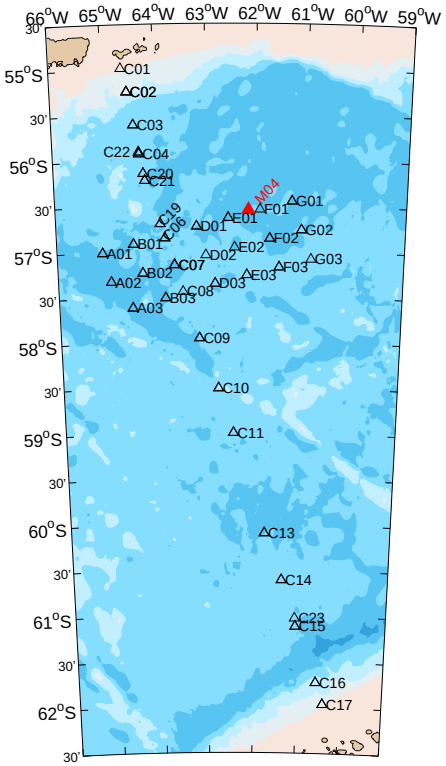

Figure 2: Location of mooring (M04) in the cDrake array is indicated by the red triangle. Black triangles indicate the locations of CPIES sites. Bathymetry derives from Smith and Sandwell (1997) contoured every 1000 m depth. Colors transition from tans representing shallow depths to light and darker blues representing successively greater depths. See *Chereskin et al.* [2009] for details of the cDrake experiment.

Level	Type	SN	Start Date Start Time	End Date End Time	Sampling Interval (min)	Averaging Interval (min)
1	Aanderaa RCM11 tilt correction off	153	19 Nov 09 12:00	last good data 18 Sept 10	30	30 (spread)
2	VMCM	069	19 Nov 09 16:08	6 Nov 10 15:49	1	1
3	Aanderaa SEAGUARD tilt correction on	137	18 Nov 09 19:59:45	31 Oct 10 02:01:28	30	1 (burst)
4	Aanderaa RCM11 tilt correction on	143	19 Nov 09 12:00	last good data 14 Sept 10	30	30 (spread)
5	Aanderaa SEAGUARD tilt correction off	136	18 Nov 09 18:53:20	31 Oct 10 02:24	30	1 (burst)
6	VMCM	002	19 Nov 09 15:39	6 Nov 10 14:49	1	1
7	Aquadopp	1395	18 Nov 09 21:35:47	last data 20 Jun 10	30	2 (burst)

Table 1: Timing information for full records, from startup prior to deployment until last data record. All times are UTC. The Aquadopp stopped recording in June 2010 due to battery failure, and both RCM11s stopped recording in September 2010 due to improper power consumption calculations. (See Table 4 for on-bottom times.) Sampling interval refers to the time between samples. Averaging interval refers to the time during which measurements are made.

	RCM11	VMCM	SEAGUARD	Aquadopp
Manufacturer	Aanderaa	WHOI	Aanderaa	Nortek
Firmware	N/A	VMCM2 V3.10	1.4.33	1.21
Current Speed				
Type	Acoustic (Doppler)	Mechanical	Acoustic(Doppler)	Acoustic (Doppler)
Range (cm s^{-1})	0 to 300	2 to 400	0 to 300	0 to 300
Accuracy (cm s^{-1})	±0.15 or ± 1%	± 1%	±0.15 or ± 1%	±0.5 or ± 1%
Resolution (cm s^{-1})	0.3	0.17	.01	.01
Direction				
Type	Hall-element compass	Flux-gate	3-axis solid-state magneto-resistor	Magnetometer
Model		TCM2-20		Nortek
Accuracy (°)	±5° (0 to 15° tilt) ±7°(15 to 35° tilt)	±3°	±5° (0 to 15° tilt) ±7.5°(15 to 35° tilt)	±2°(tilt < 20°)
Resolution (°)	0.35°	±0.1°	.01°	0.1°
Temperature				
Type	Thermistor			Thermistor
Range (°C)	-3.01 to 5.92 °C Arctic		-4 to 36°C	-4 to 40°C
Accuracy (°C)	±0.05 °C	0.01°C	±0.03°C	0.1°C
Resolution	0.1% of range		0.001°C	0.01°C
Length (mm)	595	2560	368	625
Weight (kg)	26.5	34.5	15.7	7.6

Table 2: Current meter specifications. Further information for the SEAGUARD can be found at www.aadi.no/Aanderaa/Document%20Library/1/Data%20Sheets/Seaguard%C2%AE%20RCM.pdf and for the Aquadopp at www.nortekusa.com/lib/data-sheets/datasheet-aquadopp-6000m.

SEAGUARD SN	137	136
Z-pulse DCS SN	245	244
Pressure SN	247	249
Conductivity SN	230	255
Oxygen SN	158	157

Table 3: Serial numbers for Anderaa SEAGUARD sensors. Both instruments were configured for burst mode. SN 137 (SN 136) was configured with tilt correction on (off).

3 Data Return, Clock Drift, Conversion to Scientific Units

3.1 Data Return

Current measurements were made during a 337 day period from 24 November 2009 to 28 October 2010 with the VMCMs and SEAGUARDs. For reasons noted earlier, the Aquadopp data record ended in June 2010, and the two RCM11s records ended in September (Figure 3 and Table 1). Ten days prior to the end of the Aquadopp record, the sampling interval began alternating between 12 and 30 minutes, leading us to truncate those final 10 days of Aquadopp data.

All data sets were truncated to retain only the interval when the mooring was anchored to the seafloor (Table 4). Timebases in decimal days referenced to January 2009 were assigned. The RCM11 instruments exhibited 2-minute drifts internally and their sampling intervals were adjusted to account for the drifts. The VMCMs had drifts of 7–8 minutes, based upon rotor spin-times recorded and compared to logged UTC. The time associated with the last record was changed to agree with UTC aboard ship, and their sampling intervals were adjusted. Further details of the clock drift adjustments for the RCM11s and VMCMs are given below. The SEAGUARD clocks did not drift more than a few seconds, so no timing corrections were made. We could not quantify clock drift for the Aquadopp by comparison with UTC aboard ship. However, by subsequent comparison with the SEAGUARD data (treated in Section 3.4) we estimate the Aquadopp clock drift to be 8 minutes.

Equivalent clock drifts were calculated as $\frac{\Delta t}{t}$ where Δt is the difference between the actual sampling interval and the nominal sampling interval (30 minutes for RCM11s, SEAGUARDs, and Aquadopp and 1 minute for VMCMs) and t is the nominal sampling interval (Table 4).

All data variables recorded in the raw files are listed in Table 5. No corrections have been made for magnetic declination for the intercomparison purposes of this report. All records would have identical declination.

The SEAGUARD at level 3 (SN 137) reported a mean signal strength of -52.4 dB, with standard deviation of 4.0 dB. The SEAGUARD at level 5 (SN 136) had similar signal values, respectively -51.3 dB and 4.3 dB.

3.2 RCM11 Clock Drift

Data files include one time stamp line from the Data Module clock each day; these times were assumed to be correct because both RCM11 instruments ended early, preventing comparison with UTC at recovery. The last records indicated the RCM11 clocks had drifted

by ± 2 minutes. Thus, the sampling time intervals were not exactly 30 minutes and were adjusted as folllows.

The first on-bottom record was determined by knowing the time when the anchor settled on the seafloor, and was confirmed by examining the temperature time series. The last on-bottom record was the last measurement, because the records ended early. The date and time of the first and last on-bottom records were determined from the recorded time-stamps of the Data Module.

SN 143 had a sampling-time drift two minutes later for the last record than for the first record, when each is compared to the Data Module daily time stamp (Table 6). The sampling interval was increased from 30 minutes to 30.0001415 minutes (as detailed in the table) to account for this drift.

SN 153 had a sampling-time drift two minutes earlier for the last record than for the first record, when each is compared to the Data Module daily time stamp (Table 7). The sampling interval was decreased from 30 minutes to 29.9998607 minutes (as detailed in the table) to account for this drift.

3.3 VMCM Clock Drift

WHOI provided us with MATLAB mat-files of the VMCM data records. These instruments had 60 second (1 minute) sampling intervals. Clock drifts of 7–8 minutes were determined by comparing the logged event times (rotor spins, release from the bottom, etc) with those recorded in the instruments. Sampling intervals were adjusted to account for the drifts, as follows:

SN002 had an 8 minute clock drift so the time of the last on-bottom record was changed to agree with the logged information (Table 8). The sampling interval was changed from 1 minute to 1.00001644 minutes.

SN069 had a 7 minute clock drift so the time of the last on-bottom record was changed to agree with the logged information (Table 9). The sampling interval was changed from 1 minute to 1.000014385 minutes.

3.4 Aquadopp Clock Drift

The Aquadopp data ended early and its clock could not be compared with UTC upon recovery. After initial processing it was observed that the standard deviation of differences from VMCM records was a bit high. We suspected clock drift. We tested whether assumed drifts of 1 minute intervals from -13 to 5 minutes improved the covariance with the near-zero clock-drifts of the SEAGUARDs. The covariance with both SEAGUARDs was greatest at

an assumed clock drift of -8 minutes. The Aquadopp sampling interval was then changed from 30 minutes to 29.9992 minutes.

3.5 Conversion to Scientific Units

RCM11s record integer counts in the range 0-to-1023, which are converted to scientific units using the following equations and the (A, B, C, D) coefficients listed in Table 10:

$$Speed = A + B * counts_{speed} \tag{1}$$

$$Direction = A + B * counts_{dir} \tag{2}$$

$$Temperature = A + B * counts_T + C * {counts_T}^2 + D * {counts_T}^3 \tag{3}$$

The VMCM records were converted to scientific units in the initial processing step by WHOI. The SEAGUARD and Aquadopp do the conversions to scientific units internally.

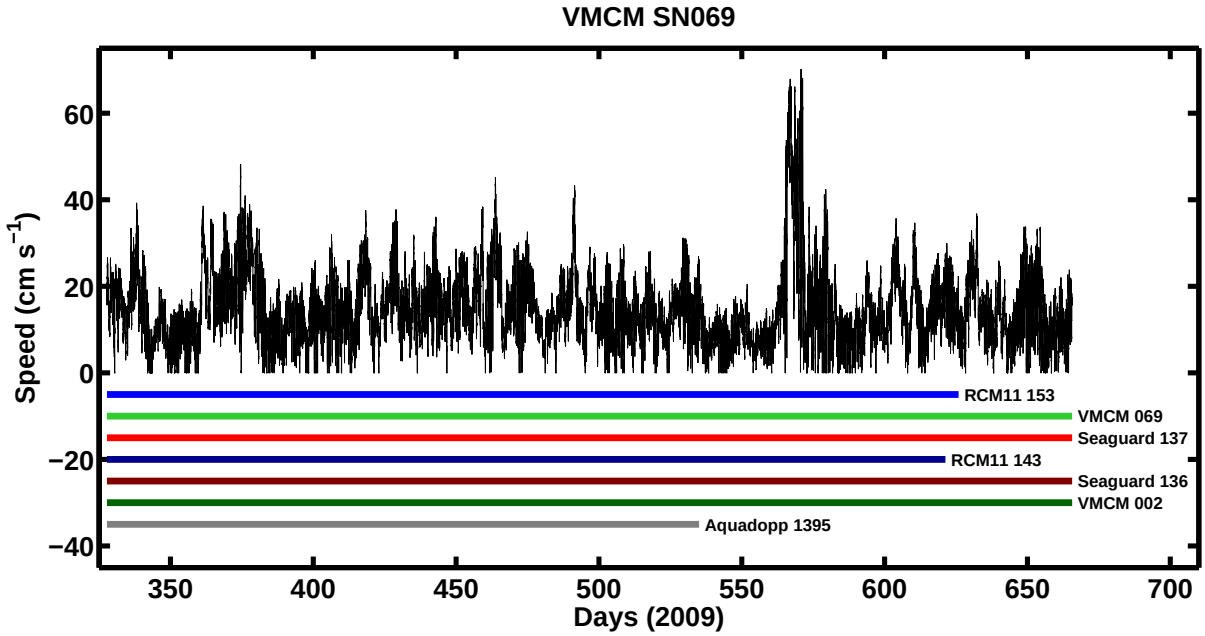

Figure 3: Top black line: Time series of VMCM SN 069 speed (cm s^{-1}). The VMCM SN 069 time base has been corrected for clock drift. Bottom colored lines: length of data records for individual current meters. The lines are plotted in order of vertical level on the mooring.

Level	Type	SN	Start DD	Start Date Start Time	End DD	End Date End Time	No. Records Length (hrs)	Clock Drift ($\frac{\Delta t}{t}$)
1	Aanderaa RCM11 tilt correction off	153	327.7694	11/24/09 18:28:00	625.9139	9/18/10 18:21:56	14312 7156	-4.6 E-6
2	VMCM	069	327.7564	11/24/09 18:09:15	665.6807	10/28/10 16:20:15	486605 8110	14.4 E-6
3	Aanderaa SEAGUARD tilt correction on	137	327.7719	11/24/09 18:31:28	665.6677	10/28/10 16:01:28	16220 8110	-12 E-12
4	Aanderaa RCM11 tilt correction on	143	327.7701	11/24/09 18:29:00	621.3132	09/14/10 07:30:59	14091 7045	4.7 E-6
5	Aanderaa SEAGUARD tilt correction off	136	327.7671	11/24/09 18:24:41	665.6630	10/28/10 15:54:41	16220 8110	-23 E-12
6	VMCM	002	327.7564	11/24/09 18:09:15	665.6807	10/28/10 16:20:15	486604 8110	16.4 E-6
7	Aquadopp	1395	327.7540	11/24/09 18:05:47	535.0508	06/20/10* 01:13:06	9962 4981	-26.7 E-6

Table 4: Serial number, start and end times for on bottom records, number of records and record length in hours and equivalent clock drift. All times are UTC. DD refers to decimal days referenced to 1 January 2009. Four of the seven currents meters (2 VMCM and 2 SEAGUARD) returned full data sets for the entire 11 month deployment. The Aquadopp stopped recording in June 2010 and both RCM11s stopped recording in September 2010.

* Note: For comparison purposes the last 10 days of the Aquadopp record were truncated because the sampling interval alternated between 12 and 30 minutes during this period.

Level	Type	SN	Speed	Direction	U, V	Temp	Compass	Tilt	Prs
1	Aanderaa RCM11 tilt correction off	153	X	X		X			
2	VMCM	069			X	X	X	X	
3	Aanderaa SEAGUARD tilt correction on	137	X	X	X	X	X	X	X
4	Aanderaa RCM11 tilt correction on	143	X	X		X			
5	Aanderaa SEAGUARD tilt correction off	136	X	X	X	X	X	X	X
6	VMCM	002			X	X	X	X	
7	Aquadopp	1395			X	X	X	X	X

Table 5: Variables recorded by current meters. The tilt recorded by the SEAGUARDs is the last tilt measured during the sampling interval, not the average tilt. For the VMCMs tilt is the last reading for each minute. Although RCM11 SN 143 applied an internal tilt correction, neither RCM11 recorded tilt.

On-bottom	Date	Time (UTC)	Record number	Decimal Day 2009
first record	24 Nov 2009	18 29 00	254	327.770138
last record	14 Sep 2010	07 31 00	14344	621.31319
			Number of Records	Elapsed Days
			14091	293.5431
				Elapsed Minutes
				422701.99488
Sampling interval = elapsed minutes / (nrec-1) = 422701.994888/14900 = 30.0001415				

Table 6: RCM11 SN143 timing information for determining clock drift.

On-bottom	Date	Time (UTC)	Record number	Decimal Day 2009
first record	24 Nov 2009	18 28 00	254	327.776944
last record	18 Sep 2010	21 56 00	14565	625.913889
			Number of Records	Elapsed Days
			14312	298.1444
				Elapsed Minutes
				429328
Sampling interval = elapsed minutes / (nrec-1) = 429328/14311 = 29.9998607				

Table 7: RCM11 SN153 timing information for determining clock drift.

event	date	log time	instrument time	offset
released	28 Oct 2010	1620–1621	1612	7–8 mins
rotor spins	6 Nov 2010	1425–1429	1417–1421	8 mins
battery unplugged	6 Nov 2010	1449	1441	8 mins

On-bottom	Date	Time (UTC)	Record number	Decimal Day 2009
first record	24 Nov 2009	18 09 15	7359	327.75642
last record	28 Oct 2010	16 20 15	493962	665.68073
			Number of Records	Elapsed Days
			486604	337.92431
				Elapsed Minutes
				486611
Sampling interval = elapsed minutes / (nrec-1) = 486611/486603 = 1.00001644				

Table 8: VMCM SN002 timing information for determining clock drift.

event	date	log time	instrument time	offset
released	28 Oct 2010	1620–1621	1614	7–8 mins
rotor spins	6 Nov 2010	1533–1535	1526–1528	7 mins
battery unplugged	6 Nov 2010	1549	1542	7 mins

On-bottom	Date	Time (UTC)	Record number	Decimal Day 2009
first record	24 Nov 2009	18 09 15	7317	327.75642
last record	28 Oct 2010	16 20 15	493921	665.68142
			Number of Records	Elapsed Days
			486605	337.925
				Elapsed Minutes
				486612
Sampling interval = elapsed minutes / (nrec-1) = 486611/486604 = 1.000014385				

Table 9: VMCM SN069 timing information for determining clock drift.

RCM11 SN	143	153
Speed Coefficients		
A	0	0
B	0.2933	0.2933
Direction Coefficients		
A	0	0
B	0.3516	0.3516
Temperature Coefficients		
A	-3.057	-3.006
B	0.009113	0.00895
C	-3.476e-007	-3.476e-007
D	1.134e-010	1.134e-010

Table 10: Calibration coefficients for RCM11s, for equations 1, 2 and 3 in Section 3.5.

4 Data Processing

4.1 Raw Data

We will start by examining the data prior to corrections for sound speed and tilt. The time stamps had been adjusted for clock drift, as described previously, which is an essential step for comparing simultaneous measurements.

The raw data show similar u and v components, as illustrated in the two highest-speed 50-day segments (Figure 4 (days 335–385) and Figure 5 (days 535–585)). Maximum speeds of approximately 48 cm s^{-1} were recorded between days 335 and 385 (Figure 4) for all seven current meters. Maximum speeds of approximately 70 cm s^{-1} were recorded between days 565 and 572 (Figure 5) for six of the current meters; the Aquadopp record ended on day 535 prior to this highest-speed event.

During the period common to all instruments, mean current speeds were approximately 9 cm s^{-1} directed to the northwest (Figure 6 top left and Table 11). The current direction of the Aquadopp and VMCM SN 069 were turned, respectively, 6° and 3° to the left of the median of all the current meters. The direction on VMCM SN 002 was turned about 8° to the right of the median. The RCM11 and SEAGUARD pairs recorded mean directions that agreed within 1 degree of their same-model partner, and all four clustered within 2 degrees of the median.

The VMCM, SEAGUARD and RCM11 pairs recorded mean speeds that ageed within 1% with their same-model partner. The two VMCMs were at the median speed of all seven current meters. The two SEAGUARD mean speeds were about 4% higher than the median. The two RCM11 mean speeds were about 6% lower than the median (Figure 6 top left and Table 11). The raw Aquadopp mean current speed was higher than the median by about 7%. We will comment upon these observed speed and angle differences after data corrections for tilt and sound speed.

Pressure was measured by the SEAGUARDs and Aquadopp (Figure 7a). The largest draw-down of the mooring (45 m) occurred during the highest current event recorded between days 565 and 572. In four other events the draw down was 20 m, but in most events the draw down was less than 10 m.

4.2 Data Corrections

Next we compare the same-model instruments within the three model pairs to verify their consistency, *i.e.*, VMCM 002 with VMCM 069, RCM11 143 with RCM11 153, and SEAGUARD 136 with SEAGUARD 137. We subsequently inter-compare the four model

types. A number of data corrections were made in preparation for these comparisons, as will be detailed in the next few subsections:

1. sound speed is corrected for the Doppler type instruments that used a constant sound speed (RCM11s and SEAGUARDs);

2. a tilt correction is applied to the current meters that were not configured to internally correct for tilt (both VMCMs, RCM11 153, and SEAGUARD 136);

3. the one-minute VMCM data are 30-minute low-pass filtered;

4. all data are expressed in components (u, v) for temporal interpolation to a synchronous 30-minute time base (UTC times, 00 and 30 minutes after each hour). Speed and direction are re-calculated afterwards.

After these corrections were made, the vectors were replotted (Figure 6, lower left) and statistics were recalculated (Table 12). Data for the two highest speed events were also examined in detail (right side of Figure 6 and Tables 13-14).

4.2.1 Sound Speed

The RCM11s and SEAGUARDs had been configured to use a constant nominal sound speed (1500 m s^{-1}) to calculate current velocity. The Aquadopp obtains the speed of sound by assuming a nominal salinity (set to 35.0 ppt here) and uses a look-up table to determine the sound speed based on the measured temperature. A data conversion function in the Aquadopp firmware calculates the speed of sound using the pressure data and corrects the velocities by applying a scale factor. In the Aquadopp header file the "sound speed" is the speed of sound initially used by the instrument when measuring, while the "sound speed used" is the pressure-corrected speed of sound used to correct the velocities in the data conversion.

The temperature records of all the CMs are consistent with each other and with four CTDs near beginning and end of the records (Figure 8 top). Temperature measurements all agreed within 0.04°C of the median of the mean temperatures (Table 11), well within the expected accuracy (Table 2).

Sound speed time series were calculated using the SEAGUARDs' pressure and temperature measurements and assuming a salinity of 35 ppt for comparison with the Aquadopp record. All three sound speed records were consistent within 0.5 m s^{-1} of each other and with those calculated from the (S, T, P) measured by the four CTDs at the beginning and end of the deployment (Figure 8 bottom). The total range of variation during the 11 months was 2 m s^{-1} , and that occurred at about the same time as the biggest current event.

Using the Doppler formula, an error in sound speed δC produces an error in current speed δU where

$$\delta \mathrm{U} \;=\; \frac{\delta \mathrm{C}}{\mathrm{C}} \;\times\; \mathrm{U} \tag{4}$$

The mean sound speed for the Aquadopp for days 327 to 525 was 1521.2 m s^{-1}. A mean value C=1521 m s^{-1} is representative of all the data.

If we use constant C=1521 m s^{-1}, then $|\delta \mathrm{C}| < 2$ m s^{-1}, and for $\mathrm{U}_{max} = 70$ cm s^{-1} then

$$\delta \mathrm{U} \;=\; \frac{2}{1521} \;\times\; 70 \text{ cm s}^{-1} \;=\; 0.09 \text{ cm s}^{-1} \tag{5}$$

which is a negligible error of 0.1%. We therefore used a constant C=1521 m s^{-1} for the RCM11s and SEAGUARDSs and scaled their current speeds larger by approximately 1.4% as follows

$$\text{current speed}_{\text{corrected}} \;=\; \text{current speed}_{\text{measured}} \;\times\; \frac{1521\,\text{m s}^{-1}}{1500\,\text{m s}^{-1}} \tag{6}$$

4.2.2 Tilt

RCM11 SN 143, SEAGUARD SN 137, and the Aquadopp current meter were configured for internal tilt correction. Tilt was recorded by the VMCMs, SEAGUARDs and Aquadopp, but not by the RCM11s (Table 5). Recall that the tilt-magnitude records were plotted in Figures 4 and 5, where tilt can be seen to systematically increase from the upper to lower current meters, as is consistent with the design of the mooring.

To apply a tilt correction to the records from the two VMCMs, RCM11 SN 153 and SEAGUARD SN 136, we calculated the tilt magnitude (ϕ) as

$$\phi = \arctan \sqrt{\tan^2(\text{tilt}_\text{x}) + \tan^2(\text{tilt}_\text{y})} \tag{7}$$

where tilt$_x$ and tilt$_y$ are the tilts recorded by the current meters.

Figure 7b shows the total tilt ϕ for both VMCMs. Mooring tilt and tilt difference were largest ($\approx 25°$, 10° respectively) during the high speed event (days 565–572).

The tilt-compensated speed, speed$_c$, was calculated as

$$\text{speed}_\text{c} = \frac{\text{speed}}{\cos\phi} \tag{8}$$

where of course the ϕ and speed time series must be synchronous. These are intrinsically synchronous for the VMCMs and the SEAGUARD, which record tilt and currents every measurement interval. The synchronization procedure for the RCM11 153 is described next. This method of speed adjustment for tilt works well for this short mooring with closely

spaced current meters, because the direction of flow was essentially independent of depth at the heights of the seven current meters, so the drag and direction of tilt were assumed to be in approximately the the same direction. Consequently, the above correction for tilt magnitude was applied to speed, rather than attempting to correct individual velocity components for each respective component of tilt.

For RCM11 153 at level 1 which did not record tilt we used ϕ calculated at level 2 for VMCM 069 in Equation 8. Subsection 4.2.4 describes how this synchronization was tailored to RCM11 153. This would be a slight overestimate of tilt for level 1, and the cosine correction factor would be only 1% different ($\cos(6)/\cos(10) = 1.010$) during even the most extreme tilt events. This would have tended to exaggerate the RCM11 153 highest speeds by 1%. For speeds less than 40 cm s^{-1} the total tilt correction increases the RCM11 153 speed by less than 0.4%, and the associated overestimate is less than 0.2%.

Details about tilt. For the RCM11, when set to internally correct for tilt, the current meter applies the tilt correction to every single ping based on the high frequency tilt measurements (Victoria, personal communication). The SEAGUARD on the other hand measures tilt at 35 kHZ, calculates an average at 1 Hz, and then applies the correction based on this average to the last second of data. However, the tilt value reported by the SEAGUARD is only the last tilt measured during the sampling interval, not the average tilt, so it may not be representative of the entire interval. Later versions of the SEAGUARD firmware correct this by providing additional tilt statistics to the QA data list. Therefore tilt compensation that we applied in post-processing may be slightly different from what the SEAGUARD does when compensating for tilt on its own (Victoria, personal communication).

For VMCMs the compass and rotors are read once per second to build a 1-minute vector average. However, the recorded tilt data is the last reading of each minute (Allsup, personal communication).

4.2.3 Lowpass filtering

The VMCM data were recorded at one-minute intervals. A fourth order lowpass Butterworth filter with a cutoff period of 30 minutes was applied to the VMCM u and v records. The filter was run forward and backward to eliminate phase offsets and data were output at 1-minute resolution.

For the other three models, whose sampling interval was 30 minutes, the preliminary data comparisons use unfiltered records. Later to determine if filtering improved the intercomparisons all data were 3-hr low pass filtered.

4.2.4 Synchronization and Interpolation

To facilitate intercomparison, it was necessary to synchronize the u and v timebases. This was accomplished in two steps. First, the recorded time stamps were shifted to correspond to the midpoints of the respective averaging intervals (see Table 1) for each model type. For the RCM11s, the time stamps occurred at the end of each sample. These times were shifted by -15 minutes to center them on the midpoint of each 30-minute-spread sample. Likewise, the Aquadopp time stamp occurred at the beginning of each 2-minute burst measurement and was thus shifted +1 minute to center it. No time shifts were made to the SEAGUARD (1-minute measurement interval). Second, the records for all models were interpolated to a common set of 30-minute intervals at 0 and 30 minutes UTC after the hour.

When interpolating onto a common time base, it is essential to work with current components (u, v) data, not speed and direction (U, θ), because a 360-to-0 degree wrap in angle θ does not interpolate to an intermediate value. Speed and direction were subsequently calculated from the interpolated u and v data.

As stated above, the RCM11 153 tilt correction was applied using the tilt measured by the neighboring VMCM 069, and so the tilt angles also required time synchronization. For VMCM 069 the tilt magnitudes ϕ range between 0 to 10 degrees; hence straightforward interpolation applied because they do not wrap through 0/360. The VMCM 069 tilts were averaged in the 30 minutes prior to the RCM11 153 time stamp to correspond to the averaging period of RCM11 153.

4.3 Excising rotor stalls

For special cases of comparison described below, in order to tightly restrict current comparisons to times with no rotor stalls, we have excised all 30-minute intervals within which any one of the four VMCM rotors stalled for even a single 1-minute interval. For those purposes, the VMCM data were block-averaged for only the stall-free 30-minute intervals. The numbers of rotor stalls for the VMCMs have been tabulated in Table 15. Extra panels have been added to some figures in the following sections, as noted in their captions, to illustrate the improvement by excising rotor stalls.

Level	Type	SN	Prs (dbar)	u (cm s^{-1})	v (cm s^{-1})	Speed (cm s^{-1})	Direction (°)	Temp (°C)	Ratio
1	RCM11 tilt correction off	153		-5.26	6.66	8.48	321.7	0.96	1.06
2	VMCM	069		-5.96	6.74	9.00	318.5	0.92	1.00
3	SEAGUARD tilt correction on	137	4016.2	-5.55	7.42	9.27	323.2	0.93	0.97
4	RCM11 tilt correction on	143		-5.40	6.57	8.50	320.6	0.96	1.06
5	SEAGUARD tilt correction off	136	4028.7	-5.73	7.44	9.39	322.4	0.93	0.96
6	VMCM	002		-4.43	7.61	8.80	329.8	0.89	1.02
7	Aquadopp	1395	4030.8	-6.75	7.01	9.73	316.1	0.94	0.93
	Median					9.00	321.7	0.93	

Table 11: Time-averaged statistics for the common time period (days 327–525). Clock drift corrections have been applied to the VMCM, RCM11 and Aquadopp time bases. The velocities are uncorrected for sound speed, and only corrected for tilt if done internally as noted in column 2. u (zonal velocity) and v (meridional velocity) are vector averaged. Speed and direction were calculated from the vector-averaged u and v. Direction is clockwise from magnetic north. Values correspond to vectors plotted in top left of Figure 6. The bottom row lists the median of the mean values in the column above it. The last column is the ratio of that median of mean speeds to each respective mean speed.

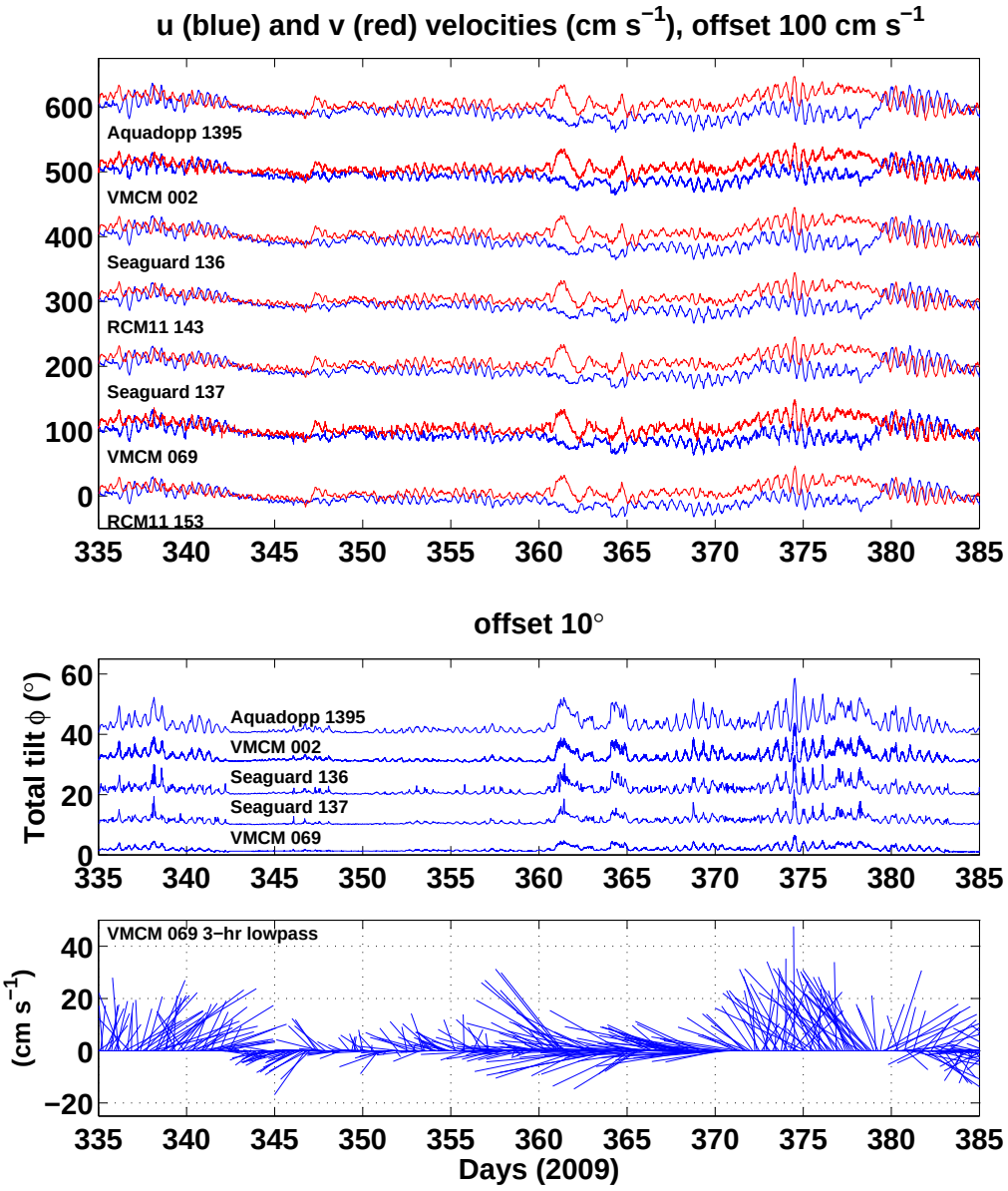

Figure 4: Top: Time series of u (blue) and v (red) velocities in cm s^{-1} for days 335–385. The shallowest current meter (RCM11 153) is plotted with no offset. Velocities for successive current meters are offset by 100 cm s^{-1}. Clock drift corrections have been applied to the VMCM, RCM11 and Aquadopp time bases. All 7 current meters were operating during this time period. Middle: Time series of total tilt for tilt-recording current meters. The shallowest tilt record is plotted with no offset, and successively deeper tilt records are offset by 10°. Bottom: Stick plot of VMCM 069 3-hr lowpass filtered velocity.

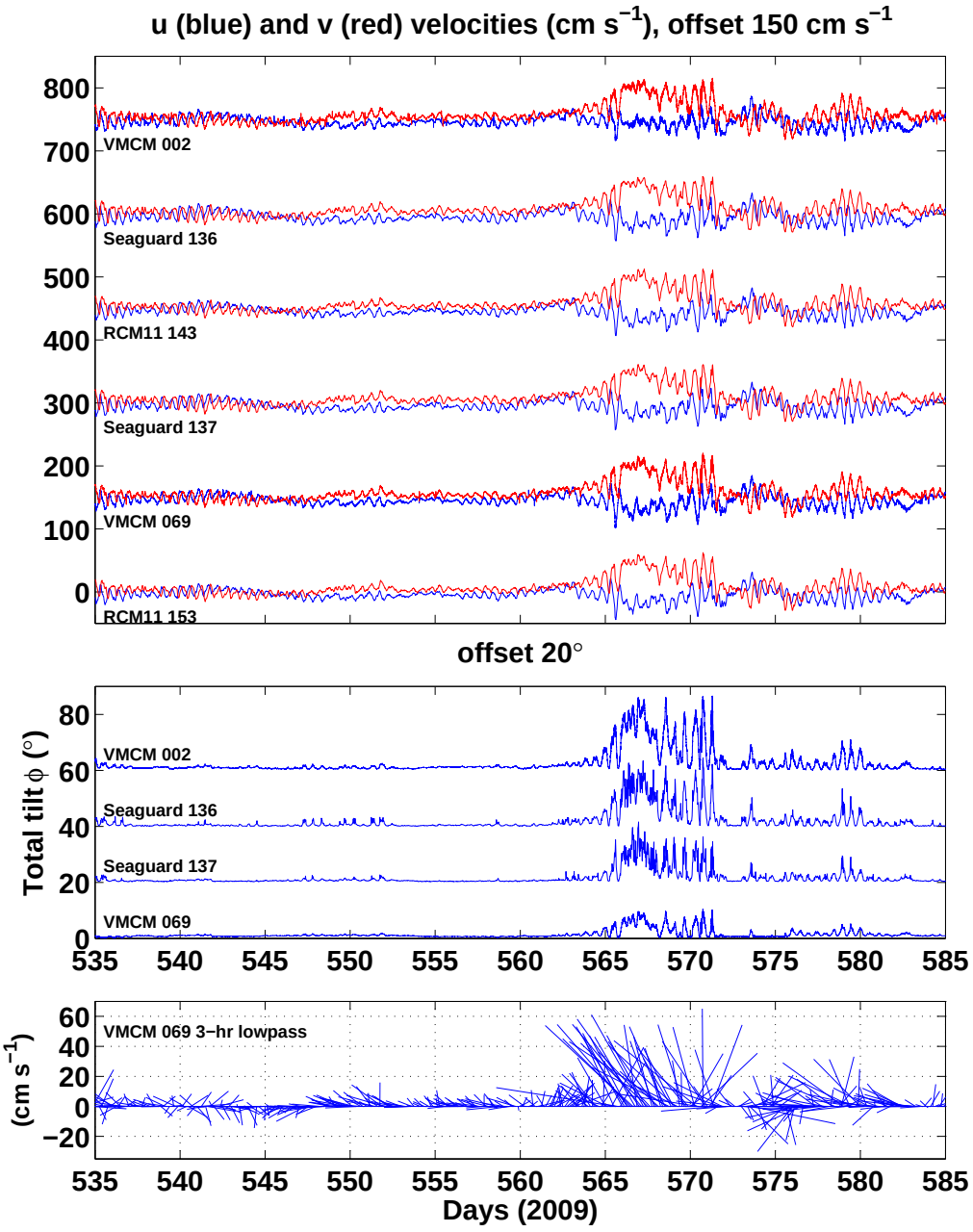

Figure 5: Time series of u (blue) and v (red) velocities in cm s^{-1} for days 535–585. The shallowest current meter (RCM11 153) is plotted with no offset. Velocities for successive current meters are offset by 150 cm s^{-1}. Clock drift corrections have been applied to the VMCM, RCM11 and Aquadopp time bases. This time period was captured by 6 of the 7 current meters and included the strongest recorded currents. Middle: Time series of total tilt for tilt-recording current meters. The shallowest tilt record is plotted with no offset, and successively deeper tilt records are offset by 20°. Bottom: Stick plot of VMCM 069 3-hr lowpass filtered velocity.

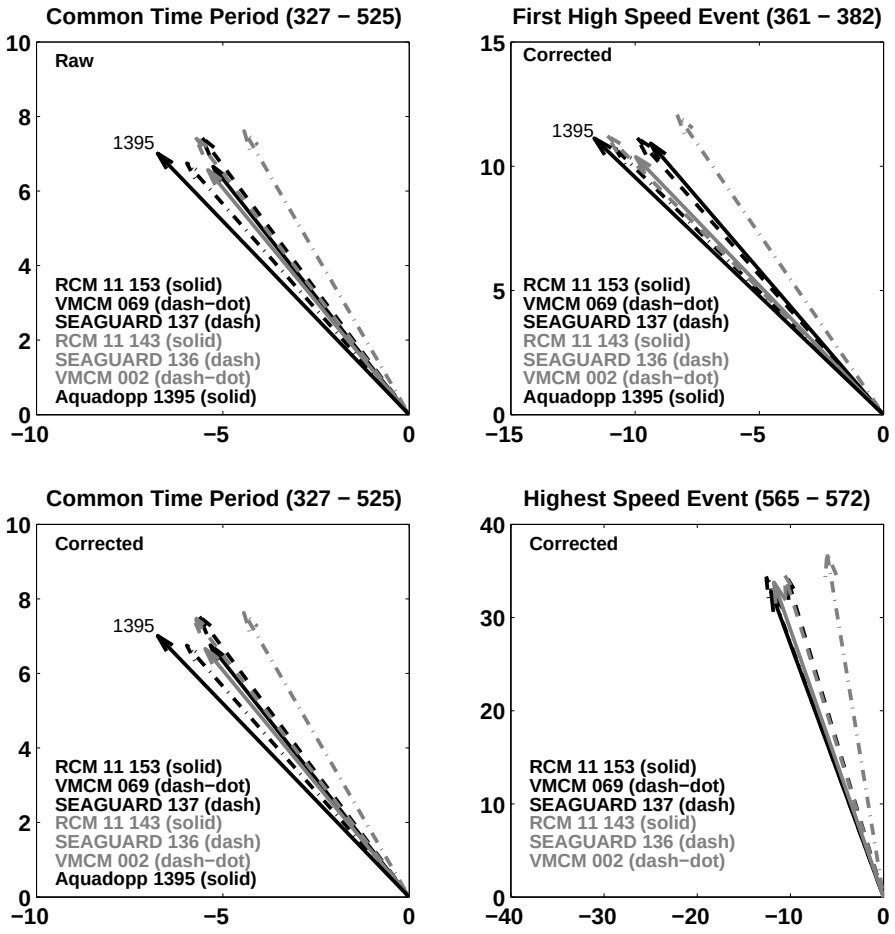

Figure 6: Time averaged velocity vectors. Top left: common time period (days 327–525). Clock drift corrections have been applied to the VMCM, RCM11 and Aquadopp time bases. RCM11 143, SEAGUARD 137 and Aquadopp 1395 data are internally compensated for tilt. The Aquadopp used a variable speed of sound calculated from measured temperature and constant salinity. In the other three panels the data have been corrected for sound speed and tilt and interpolated to a common 30-minute time base. The VMCM data were 30-minute lowpass filtered. Bottom left: days 327–525. Top right: days 327–621. Bottom right: highest speed event, days 565–572.

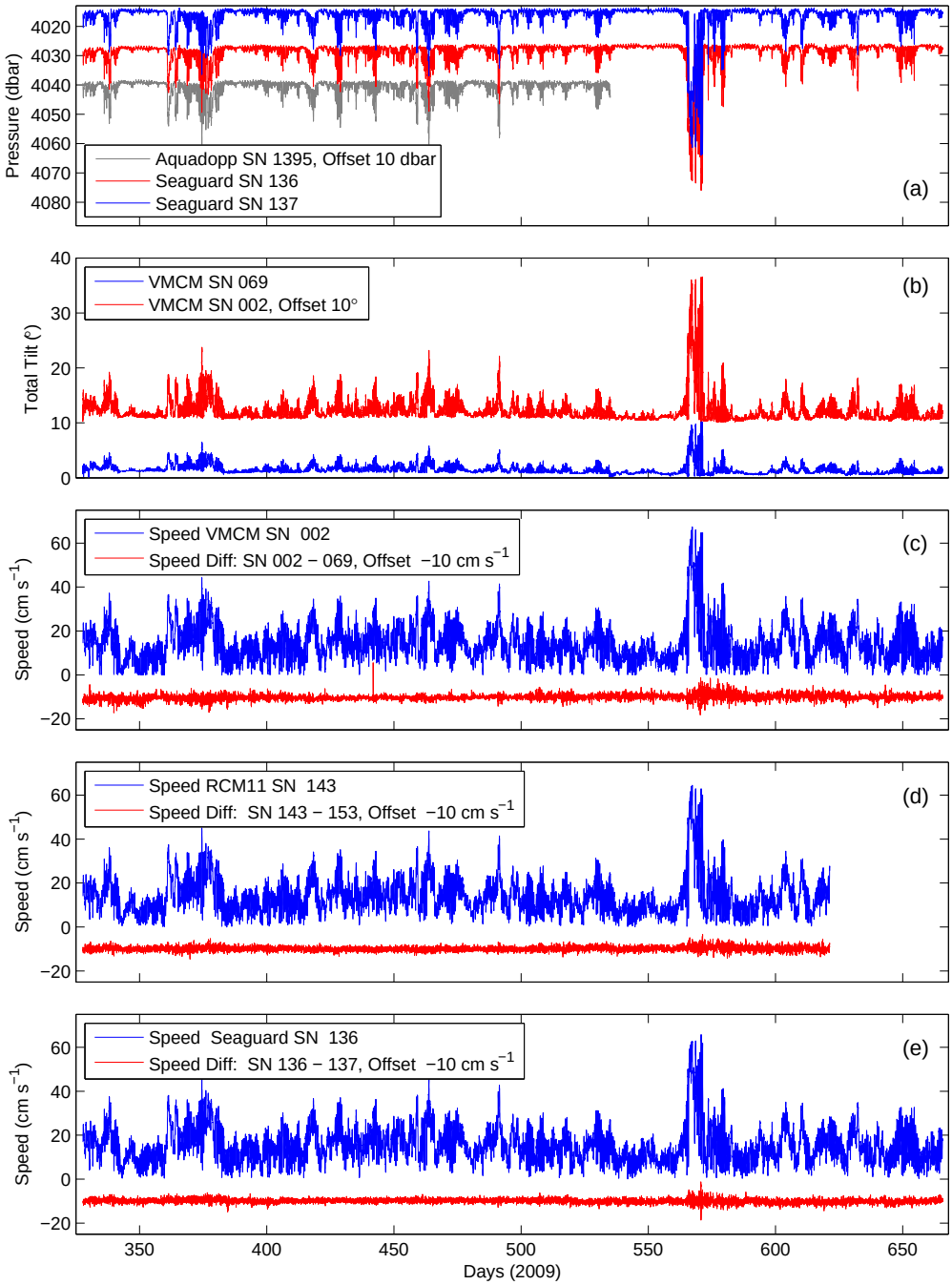

Figure 7: Pressure in dbar for SEAGUARDs and Aquadopp (a), VMCM tilts as labeled (b), and speed (blue) and speed difference (red) for VMCM (c), RCM11 (d) and SEAGUARD (e) current meters. All records have been corrected for sound speed and tilt and interpolated to a common 30-minute timebase. The VMCM data were 30-minute lowpass filtered.

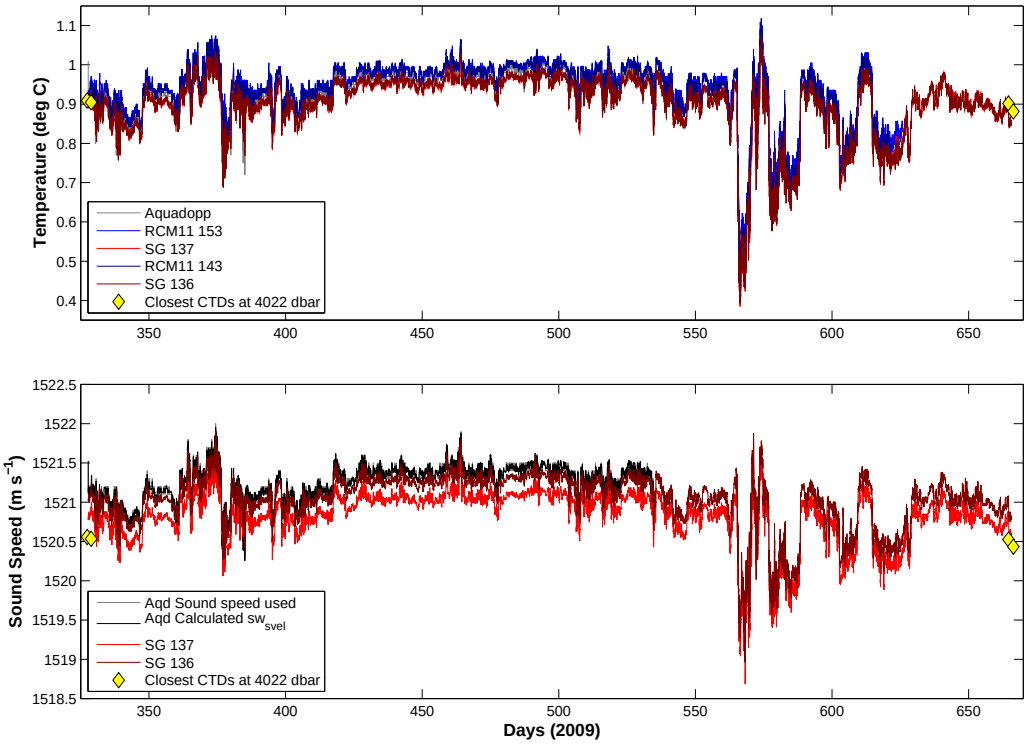

Figure 8: Top: Temperature from Aquadopp, RCM11s, SEAGUARDs, and closest CTD casts. Closest CTDs are between 8–14 nm from the mooring location. Bottom: sound speed from Aquadopp, SEAGUARDs (using measured temperature and pressure and salinity = 35 ppt) and CTDs (using measured S, T, and P).

Level	Type	SN	Prs (dbar)	u (cm s^{-1})	v (cm s^{-1})	Speed (cm s^{-1})	Direction (°)	Temp (°C)	Ratio
1	RCM11 tilt correction off	153		-5.34	6.76	8.61	321.7	0.96	1.05
2	VMCM	069		-5.97	6.75	9.01	318.5	0.92	1.00
3	SEAGUARD tilt correction on	137	4016.2	-5.63	7.52	9.40	323.2	0.93	0.96
4	RCM11 tilt correction on	143		-5.47	6.66	8.62	320.6	0.96	1.05
5	SEAGUARD tilt correction off	136	4028.7	-5.82	7.55	9.54	322.4	0.93	0.94
6	VMCM	002		-4.43	7.63	8.82	329.8	0.89	1.02
7	Aquadopp	1395	4030.8	-6.75	7.01	9.73	316.1	0.94	0.93
	Median					9.01	321.7	0.93	

Table 12: Time-averaged statistics for common period (days 327–525). Data have been corrected for sound speed and tilt and interpolated to a common 30-minute timebase. The VMCM data were 30-minute lowpass filtered. u (zonal velocity) and v (meridional velocity) are vector averaged. Speed and direction were calculated from the vector-averaged u and v. Direction is clockwise from magnetic north. Values correspond to vectors plotted in bottom left of Figure 6. The bottom row lists the median of the mean values in the column above it. The last column is the ratio of that median of mean speeds to each respective mean speed.

Level	Type	SN	Prs (dbar)	u (cm s^{-1})	v (cm s^{-1})	Speed (cm s^{-1})	Direction (°)	Temp (°C)	Ratio
1	RCM11 tilt correction off	153		-9.37	10.92	14.39	319.4	0.97	1.04
2	VMCM	069		-10.79	10.70	15.20	314.8	0.90	0.98
3	SEAGUARD tilt correction on	137	4018.9	-9.91	11.13	14.91	318.3	0.93	1.00
4	RCM11 tilt correction on	143		-9.97	10.38	14.39	316.1	0.96	1.04
5	SEAGUARD tilt correction off	136	4031.5	-11.11	11.22	15.79	315.3	0.93	0.94
6	VMCM	002		-8.30	12.08	14.66	325.5	0.85	1.02
7	Aquadopp	1395	4033.3	-11.64	11.13	16.11	313.7	0.93	0.93
	Median					14.91	316.1	0.93	

Table 13: Time-averaged statistics for the first high speed event (days 361–382). Data have been corrected for sound speed and tilt and interpolated to a common 30-minute timebase. The VMCM data were 30-minute lowpass filtered. u (zonal velocity) and v (meridional velocity) are vector averaged. Speed and direction were calculated from the vector-averaged u and v. Direction is clockwise from magnetic north. Values correspond to vectors plotted in top right of Figure 6. The bottom row lists the median of the mean values in the column above it. The last column is the ratio of that median of mean speeds to each respective mean speed.

Level	Type	SN	Prs (dbar)	u (cm s^{-1})	v (cm s^{-1})	Speed (cm s^{-1})	Direction (°)	Temp (°C)	Ratio
1	RCM11 tilt correction off	153		-12.07	32.81	34.96	339.8	0.70	1.03
2	VMCM	069		-12.60	34.41	36.64	339.9	0.67	0.98
3	SEAGUARD tilt correction on	137	4035.3	-10.31	34.21	35.73	343.2	0.66	1.01
4	RCM11 tilt correction on	143		-11.76	33.78	35.77	340.8	0.68	1.01
5	SEAGUARD tilt correction off	136	4047.3	-10.61	34.57	36.17	342.9	0.65	0.99
6	VMCM	002		-6.06	36.86	37.35	350.7	0.62	0.96
	Median					35.97	341.9	0.66	

Table 14: Time-averaged statistics for highest speed event (days 565–572). Data have been corrected for sound speed and tilt and interpolated to a common 30-minute timebase. The VMCM data were 30-minute lowpass filtered. u (zonal velocity) and v (meridional velocity) are vector-averaged. Speed and direction were calculated from the vector-averaged u and v. Direction is clockwise from magnetic north. Values correspond to vectors plotted in bottom right of Figure 6. The bottom row lists the median of the mean values in the column above it. The last column is the ratio of that median of mean speeds to each respective mean speed.

Level	VMCM SN	1-min values rotor1==0	% of total	1-min values rotor2==0	% of total	1-min values r1 or r2 ==0	% of total
2	069	20763	4.3%	32226	6.6%	47669	9.8%
6	002	26243	5.4%	5724	1.2%	30105	6.2%

Table 15: Number of VMCM rotor stalls. The total number of VMCM 069 (002) 1-minute values is 486605 (486604). There were 16,220 30-minute VMCM block averages of which 4754 (29.3%) were excised due to rotor stalls in any of the four rotors.

5 Results and Comparisons

5.1 Spectra

Spectra of u and v components are calculated and displayed two different ways. Note the spectra were calculated before the data were interpolated to a common time base (i.e, prior to step 4 in Section 4.2). The variance-conserving form in Figure 9 used the Welsh method with window length 1392 points (29 days) applied to the full record lengths (different for different instruments), to produce well-resolved spectral peaks and distinguish the tidal peaks and the local inertial period (14.4 hr at latitude 56.55°S). The two highest peaks are the semidiurnal tide (1/12.42 h = 0.08 h^{-1}) and the inertial peak at 1/14.4h = 0.07 h^{-1}; a quarter-diurnal tide peak and a broader peak near 10-to-2 days are also evident. The long-period spectra differ among the four panels because the records spanned different time intervals.

Our main interest here focuses upon the instruments. In order to compare the measurement noise-floors of the seven records during their common time period, the log-log form of spectral density in Figure 10 used the Welsh method with one-quarter the window length, 348 points (7.25 days), to produce more smoothing from ensemble-averaging. At periods shorter than 3 hours the spectral slope flattens where an apparent measurement noise floor exceeds the high frequency signal variance of currents at this location.

The measurement noise levels of the instruments are listed in Table 16. Internal tilt correction was turned off for both RCM11 153 and SEAGUARD 136; tilt for these two current meters was corrected by Equation 8. Thus within each of these two pairs of same-model instruments, the noise floor was the same regardless of whether the tilt correction was done internally or calculated in post processing. To compare their noise variance, which appeared to be isotropic, all the records were 3-hour high-pass filtered and their eddy kinetic enery, $EKE_{<3hr}$ is tabulated in Table 16. The VMCMs had the lowest noise floor. The RCM11s and SEAGUARDs have somewhat higher noise floors and the Aquadopp had the highest.

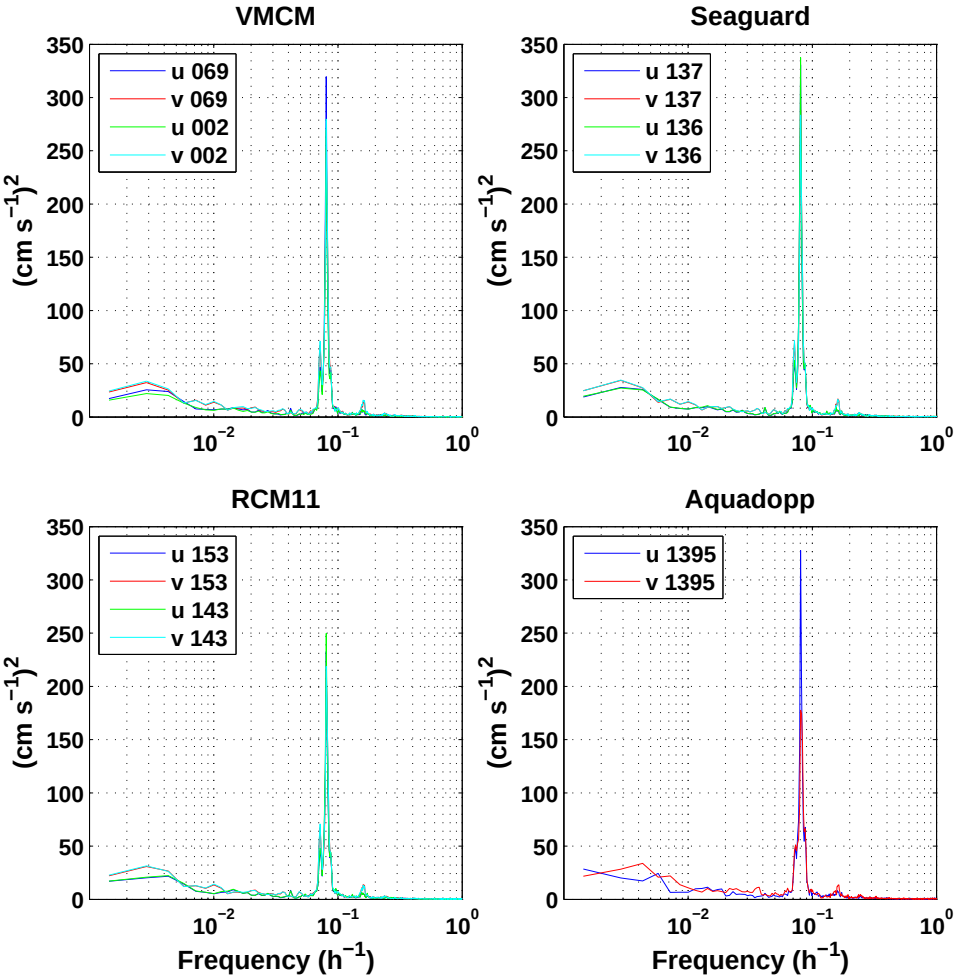

Figure 9: Variance preserving plots of spectra of full record length u and v velocities, as labeled. All records have been corrected for sound speed and tilt. The VMCM data were 30-minute lowpass filtered. A window length of 1392 points (29 days) was used for the spectra.

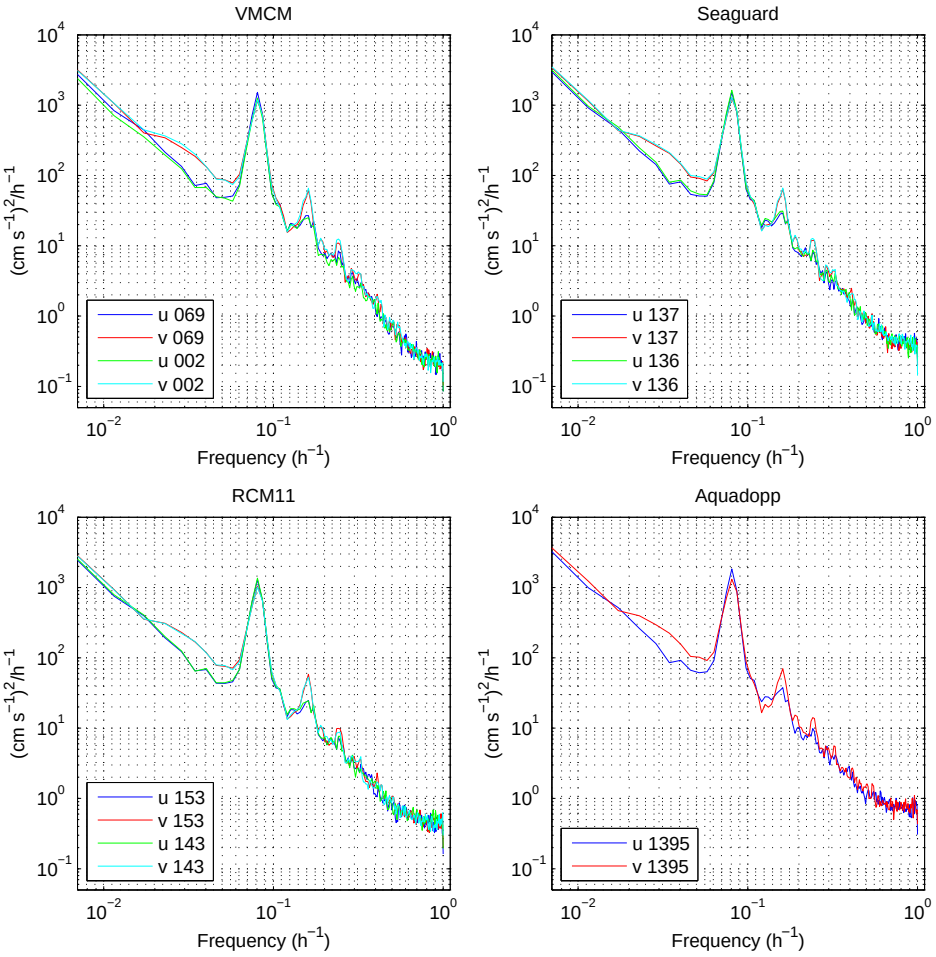

Figure 10: Spectral densities of u and v velocities for the common time period (days 327–525), as labeled. All records have been corrected for sound speed and tilt. The VMCM data were 30-minute lowpass filtered. A window length of 348 points (7.25 days) was used.

Level	Type	SN	NSD $(\mathrm{cm/s})^2/\mathrm{h}^{-1}$	$EKE_{<3hr}$ $(\mathrm{cm}^2\mathrm{s}^{-2})$	Internal Tilt Correction
1	RCM11	153	0.45	0.44	No
2	VMCM	069	0.30	0.33	No
3	SEAGUARD	137	0.45	0.45	Yes
4	RCM11	143	0.45	0.45	Yes
5	SEAGUARD	136	0.45	0.46	No
6	VMCM	002	0.30	0.33	No
7	Aquadopp	1395	0.70	0.67	Yes

Table 16: Measurement noise levels. NSD is the noise spectral density obtained from the high frequency 'tails' of the spectra in Figure 10.

5.2 Current Meter Same-Model Pair Comparisons

Time series of speed and speed differences for the same-model current-meter pairs are shown in Figure 7c (VMCM), 7d (RCM11) and 7e (SEAGUARD). Data corrections 1 to 4 (Section 4.2) have been applied to these time series. In one event around days 565–572 the peak speeds reached 67 cm s^{-1}. In that event the tilt of the lowest current meter reached about 25 degrees and the upper part of the mooring pulled down about 40 m (Figure 7a).

A close comparison of these same-model pairs is provided by scatter plots for current-direction measurements in Figure 11, and for current-speed measurements in Figure 12. Directions differ the most when speeds are less than 5 cm s^{-1} (red dots in Figure 11), especially for the VMCMs. The dots in the upper left and lower right corners in Figure 11 arise from the normal amount of scatter about the one-to-one line accounting for the wrap from 360-to-0 degrees.

The VMCM 002 direction, which was offset from the median by 8 degrees, differs from a straight line constant offset from VMCM 069. The offset depends on angle; note the slight curvature of the cloud of black dots relative to the line with unity slope. The apparent dependence on speed (Figure 11) may be indirect, because the speeds at this location were not isotropically distributed but tended to be higher or lower in certain directions. During shipboard setup, the battery for VMCM 002 was initially plugged in with the wrong polarity and a resistor burned out. A replacement resistor was found and soldered in VMCM 002. It is possible that during reassembly the compass was inadvertently turned or the momentary high current when the battery was attached incorrectly caused a magnetic field that polarized something in or near the compass. VMCM compass deviation pre- and post-deployment are shown in Figures 13 and 14. VMCM 002 shows nothing so large as an 8 degree change from

pre- to post-deployment as might have been expected if the compass had been magnetized when the battery shorted. However, because the compass of VMCM 002 disagrees with the other instruments, we have selected VMCM 069 for further comparisons with other-model current meters. The other current directions generally agreed well, *i.e.*, within their typical specifications of 5 degrees, for speeds greater than 10 cm s^{-1}, and all cases of substantially larger disagreement occurred for speeds less than 5 cm s^{-1}.

The speed comparisons (Figure 12), which are the focus of this study, agree well within same-model pairs. VMCM speeds agree with unity slope within 1%. The standard deviation difference in VMCM speed measurement was 1.06 cm s^{-1} (see Table 17 which includes different model pair comparisons also). The same-model speed comparisons for SEAGUARD measurements agree with unity slope within 2%, and standard deviation difference scatter was 0.79 cm s^{-1}. The RCM11 measurements agree with unity slope within 2% and rms difference 0.90 cm s^{-1}. We show later (Figure 27) that standard deviations have a minimum around 0.5 cm s^{-1} and increase roughly in proportion to vertical separation distance on the mooring. The statistics shown in Figure 12 panels were derived as follows: For each 30-minute pair of measurements the ratio of speeds was calculated if both exceeded a speed threshold,

$$\mathrm{r} \;=\; \left[\frac{\mathrm{speed_{cmu}} > \mathrm{st}}{\mathrm{speed_{cml}} > \mathrm{st}}\right] \tag{9}$$

where st is the lower speed threshold (5 or 10 cm s^{-1}) and cmu and cml refer to the upper and lower current meters of each model type. The mean ratio and standard error of that mean are then determined,

$$\mu_{\mathrm{st}} \;=\; \bar{\mathrm{r}} \tag{10}$$

and

$$\mathrm{ermean} = \frac{\mathrm{std(r)}}{\sqrt{(\mathrm{n}-1)}} \tag{11}$$

Scatter plots of the difference in current direction (deep direction − shallow direction) are plotted versus speed of the deeper current meter of each pair in Figure 15. The red asterisks in Figure 15 are the median direction difference calculated for 2 cm s^{-1} bins.

The fourth (lower left) panel in each of Figures 11, 12, and 15 re-compares the VMCM data after excising all 30-minute intervals in which any one of the four rotors stalled for even one minute. Table 15 shows that individual rotors stalled during 1% -to- 7% of the 1-minute sample intervals, presumably depending mainly upon orientation of the current meter housing on the mooring. The fraction of 30-minute intervals unaffected by any stall of any single rotor during any 1-minute subinterval was greater than 70%. The slightly curved deviation from constant angle offset remains the same (Figure 11), and most notably the

scatter is greatly reduced in direction differences, which had been largest for low current speeds. The VMCM current speeds continue to agree with unity slope within 1% (Figure 12).

Time series of speed and direction difference for days 535 to 585 are shown in Figures 16 and 17. These figures reemphasize that the current angles exhibit least scatter when current speeds are high.

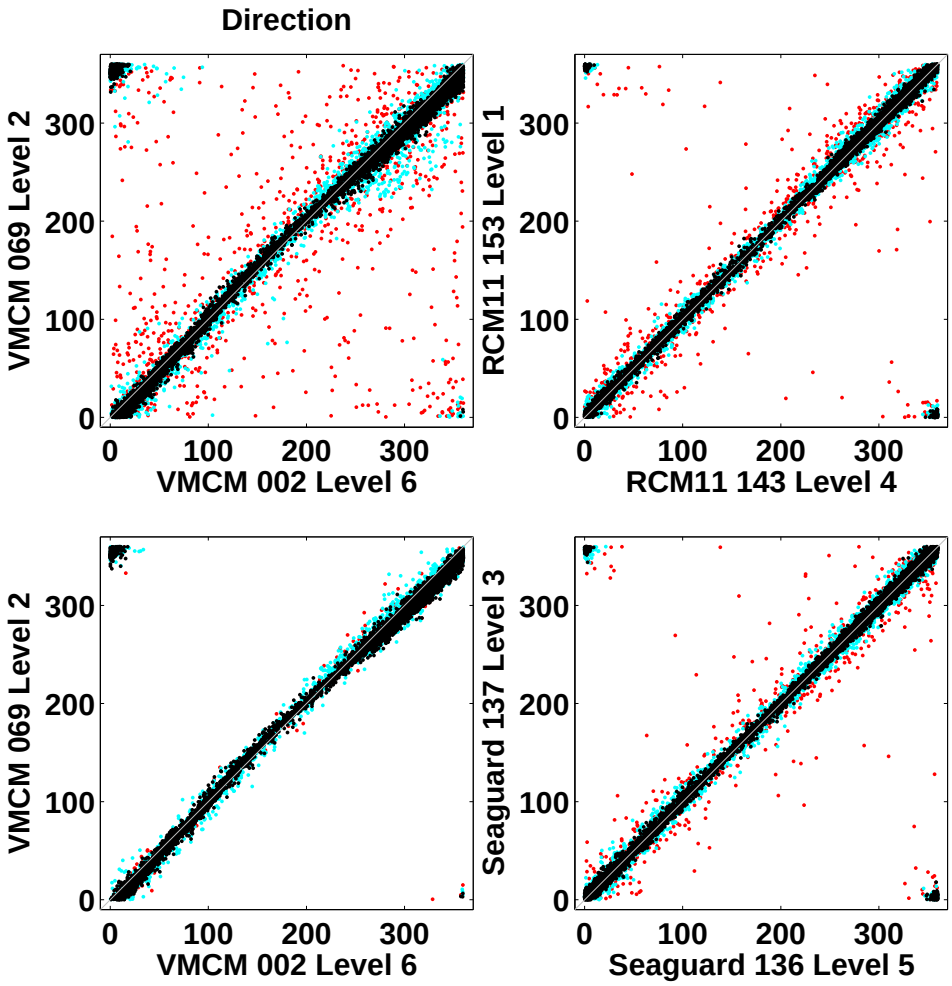

Figure 11: Scatter plots of current direction for same model current meter pairs. Red dots correspond to speeds <= 5 cm s^{-1}, cyan to speeds > 5 cm s^{-1} and <10 cm s^{-1}, and black to speeds >=10 cm s^{-1}. VMCM data in lower left panel have had all rotor stalls excised. Gray line has a slope of one.

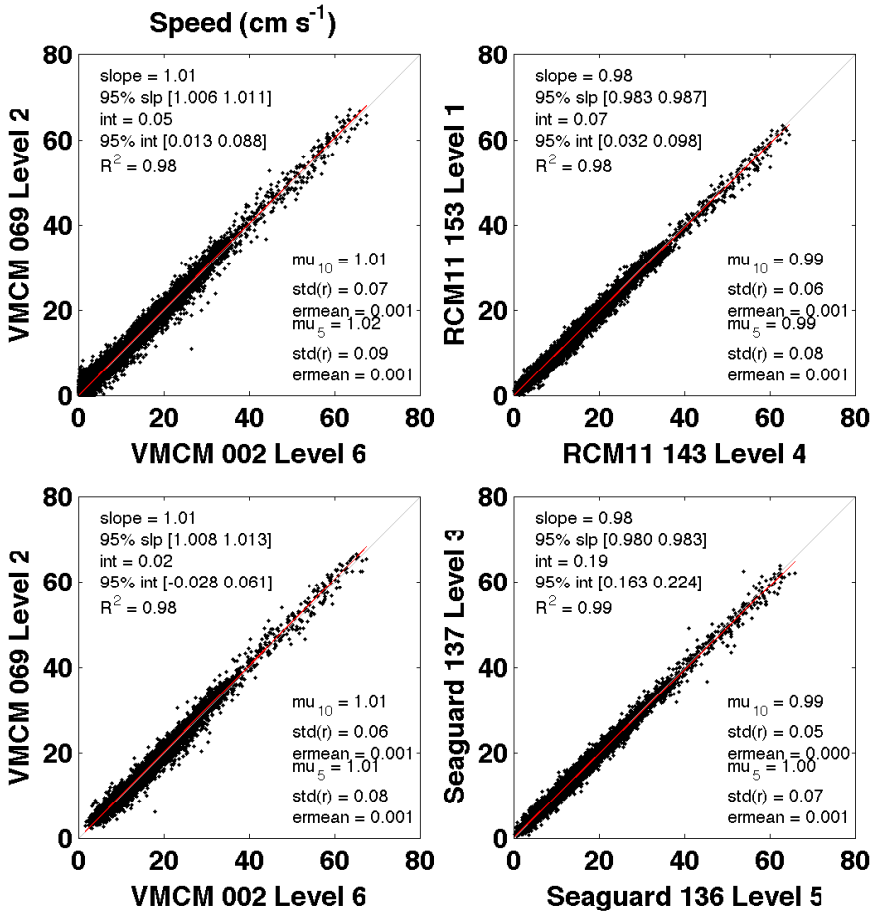

Figure 12: Scatter plots of current speed for same model current meter pairs. All records have been corrected for sound speed and tilt. Top left: VMCM 30-minute lowpass filtered and interpolated to common 30-minute timebase. Bottom left: VMCM 30-minute block averaged with rotor stalls excised. Top right: RCM11. Bottom right: SEAGUARD. RCM11 and SEAGUARD were interpolated to common 30-minute timebase. The gray line has a slope of one. The red line is the fit to the data. The slope and intercept of the red line and their confidence intervals are listed in the upper left corner of each plot. The statistics listed in the lower right corner of each plot are described in Section 5.2 where the subscripts 5 and 10 refer to the lower speed threshold used in error calculations.

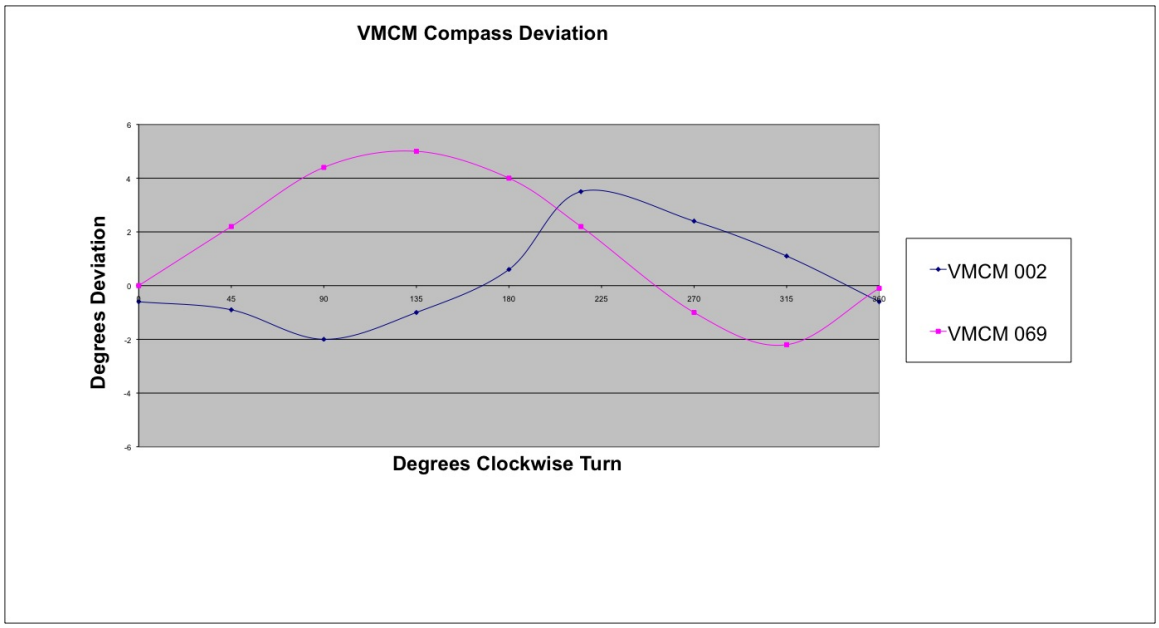

Figure 13: Pre-deployment VMCM compass deviation.

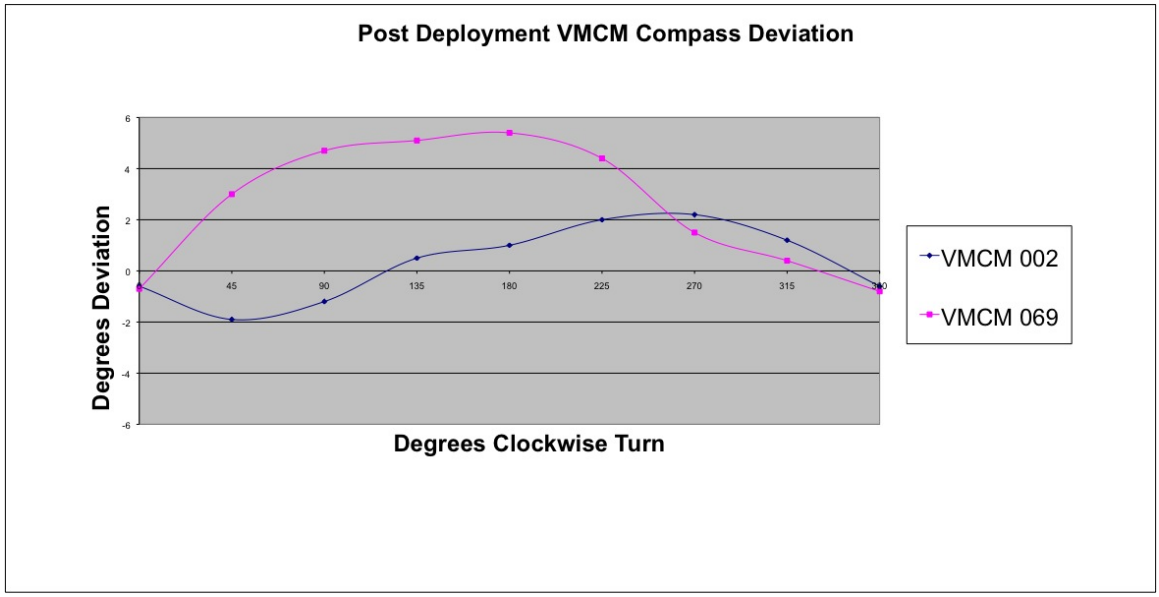

Figure 14: Post-deployment VMCM compass deviation.

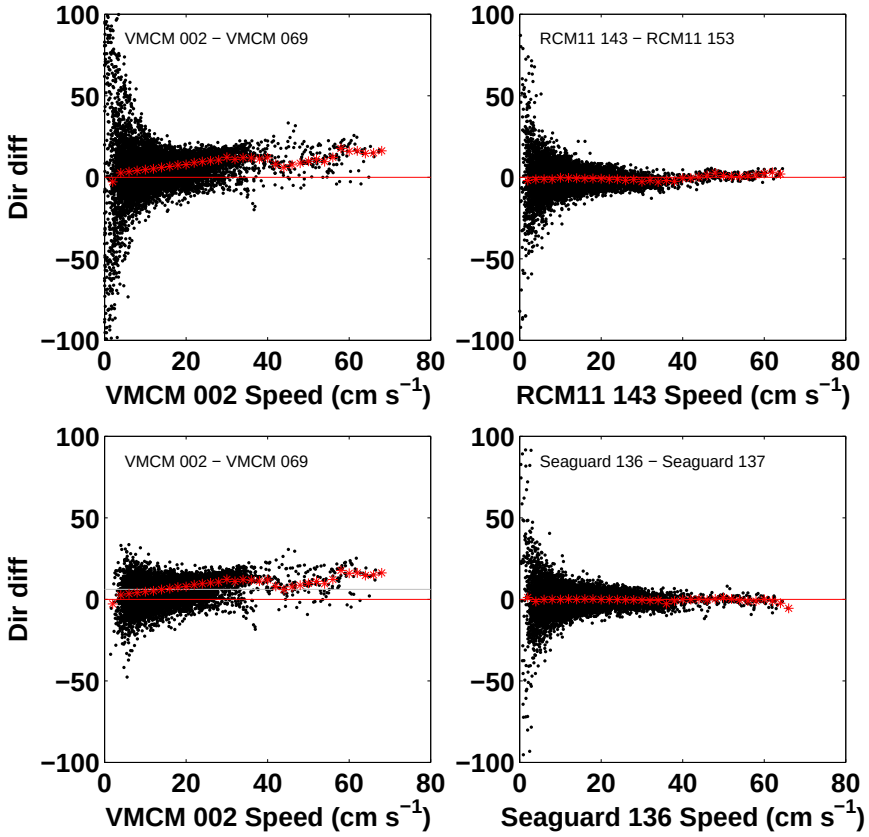

Figure 15: Scatter plots of the difference in current direction versus speed of the deeper current meter of each same model pair. All records have been corrected for sound speed and tilt. The asterisks represent the median difference calculated for 2 cm s^{-1} bins. Top left: VMCM 30-minute lowpass filtered and interpolated to common 30-minute timebase. Bottom left: VMCM 30-minute block averaged with rotor stalls excised. The mean direction difference (6.1°) for block averaged data is shown by the gray line. Top right: RCM11. Bottom right: SEAGUARD. RCM11 and SEAGUARD were interpolated to common 30-minute timebase. The standard deviations of the angle differences for speeds greater than 5 cm s^{-1} and 10 cm s^{-1} for filtered VMCM data are 7.9° and 6.1°, for RCM11s 4.9° and 3.8° and for SEAGUARDS 4.6° and 3.7° respectively. The standard deviations for block averaged VMCM data are the same as for filtered data, 7.9° and 6.1°.

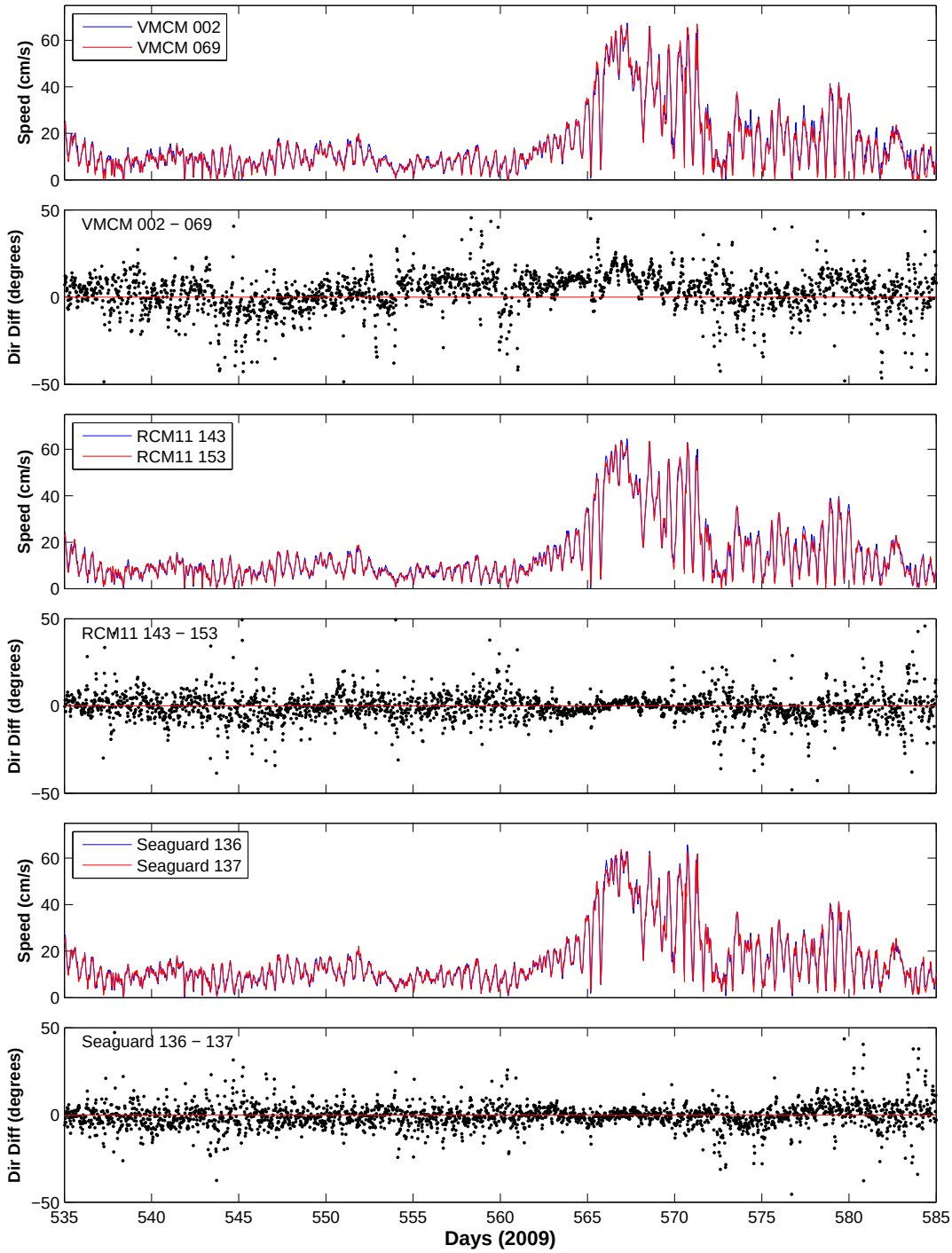

Figure 16: Time series of speed (panels 1, 3 and 5) and direction difference (panels 2, 4 and 6) for same model current meters pairs for days 535–585. All records have been corrected for sound speed and tilt and interpolated to a common 30-minute timebase. The VMCM data were 30-minute lowpass filtered.

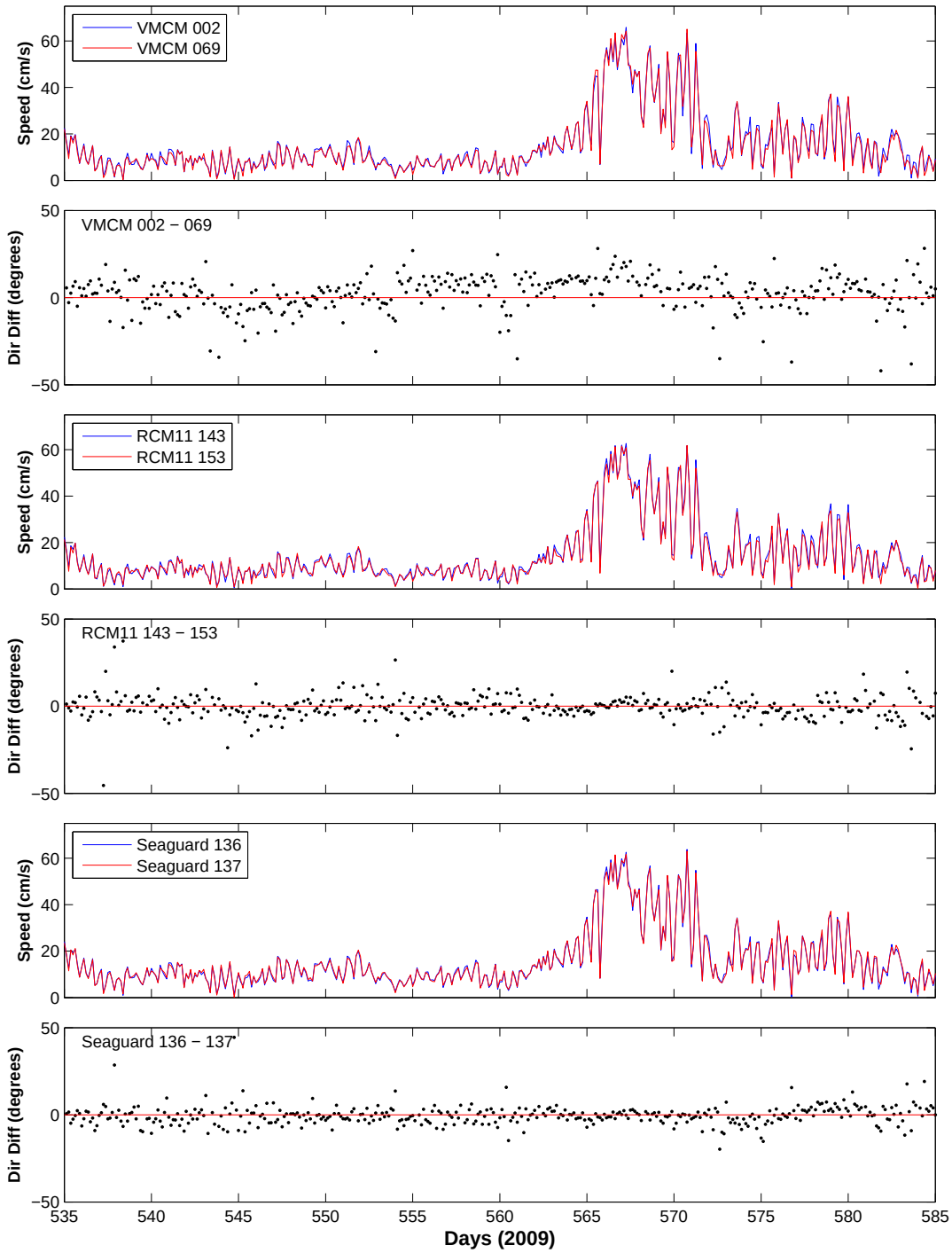

Figure 17: Same as Figure 16 except all records were 3-hour lowpass filtered.

5.3 Current Meter Different-Model Comparisons

We chose one representative from each of the current meter models for these intercomparisons. The instruments chosen were VMCM 069, RCM11 153, SEAGUARD 136 and Aquadopp 1395. VMCM 069 was chosen because the compass of VMCM 002 differed from the other instruments. Either RCM11 and either SEAGUARD could have been chosen for further intercomparison between models. We chose RCM11 153 and SEAGUARD 136 for which tilt corrections were post processed consistently with VMCM 069.

Time series of the four different current meter types, zoomed-in for 25 days during the first large-current event, are compared in Figure 18. These records have applied the four corrections listed in Section 4.2 (sound speed; tilt; 30-minute lowpass filtering VMCM; interpolation to common time base.) The speeds appear so similar that it is difficult to distinguish them in this plot. Closer comparison can be provided by the following plots and statistics.

A close comparison for current-direction measurements of the different-model pairs is provided by the six scatter plots in Figures 19 and 20, for current speed measurements in Figures 21 and 22, for direction difference as a function of speed in Figures 23 and 24 and for speed difference as a function of time in Figures 25 and 26. These plots all use the maximum coincident time series available for each respective pair of instruments. As noted earlier, the dots in the upper left and lower right corners in Figures 19 and 20 arise from the normal amount of scatter about the one-to-one line accounting for the wrap from 360-to-0 degrees. The curvature that was evident in comparing direction for the two VMCMs, 069 and 002, is absent here, offering further evidence that the problem lies with 002 and not 069.

Judged by the slopes of the scatter plots (Figure 21), the RCM11 153 speeds are 5% lower than VMCM 069 (slope 0.94), 9% lower than the Aquadopp (slope 1.09), and essentially the same as SEAGUARD 136 (slope 1.00).

The scatter plots of the difference in current direction versus speed for one current meter of each pair (Figures 23 and 24) all exhibit similar amounts of direction-scatter, and in all cases the direction-scatter decreases with increasing current speed. Direction for VMCM 069 is offset a few degrees to the left (2°–4°) of the RCM11 and SEAGUARD, and a few degrees to the right of the Aquadopp, consistent with the time-mean vector comparison (Figure 6). Direction for the Aquadopp is a few degrees to the left of all other instruments, and the RCM11 and SEAGUARD directions agree within about 1 degree with each other, again consistent with the time-mean vector comparisons.

At first impression, the time series of speed differences between current meters (Figures 25 and 26) emphasize that a fairly constant offset persists over the whole span of measurements. Referring back to the overall speed time-series plot (Figure 3) this accords with the speeds remaining fairly steady, oscillating around 5–20 cm s^{-1}, for most of the deployment. Only by

close inspection can the speed bias at high currents be discerned in these time series at the two high-speed events, highest near day 565–572 and the second-highest near days 361–382.

The time-mean and standard deviations of speed differences for the common time period (days 327–525) are listed in Table 17. The speed-difference standard deviations range between 0.7-to-1.5 cm s^{-1} between most pairs, owing partly to real turbulent velocity differences between locations on the mooring. The speed differences are also compared after 3-hour lowpass filtering each record (Table 18) in order to remove that part of their variance that was strongly influenced by measurement noise-floor (see Section 5.1). However the standard deviations were only reduced by a relatively small amount. The standard error of the mean differences would be about 0.02 cm s^{-1}, as estimated by $std/\sqrt{(DOF)}$, where DOF is degrees of freedom, with 9456 independent measurements at half-hour intervals during the common time period. The means of the half-hourly speed-differences (summarized from Table 17) are usually more than twice as large as the differences of vector-mean current magnitudes (Table 12). This may arise because noise in individual components (u, v) averages to zero, but adds to mean speed $(u^2 + v^2)^{\frac{1}{2}}$. The "noise floor" of measurement alone is insufficient to account for the difference. So part of the speed difference is oceanic (discussed later with Figure 27), and part arises from sampling-time differences as next discussed.

The two VMCM mean speeds agreed with each other within 0.43 cm s^{-1} (Table 17). The two RCM11 mean speeds agreed with each other within 0.06 cm s^{-1}, and are on average over the common time period:

- $(0.77 + 0.38 + 0.30 + 0.69)/4 = 0.5$ cm s^{-1} lower than the two VMCMs,
- $(1.74 + 2.00 + 1.68 + 1.94)/4 = 1.8$ cm s^{-1} lower than the two SEAGUARDs,
- $(2.15 + 2.09)/2 = 2.1$ cm s^{-1} lower than the Aquadopp.

The two SEAGUARD mean speeds agreed with each other within 0.26 cm s^{-1} (Table 17) and are about

- $(0.99 + 1.38 + 1.24 + 1.63)/4 = 1.3$ cm s^{-1} higher than the two VMCMs,
- $(0.41 + 0.15)/2 = 0.3$ cm s^{-1} lower than the Aquadopp.

The Aquadopp speed mean was about

- $(1.40 + 1.79)/2 = 1.6$ cm s^{-1} higher than the two VMCMs.

The finding that within same-model pairs the speed agreement is very good (0.43, 0.06, 0.26 cm s^{-1}) compared to different-model pairs (ranging 0.15 to 2.15 cm s^{-1}) suggests that some of the difference arises from sampling differences within each half-hour. This idea is

supported by the fact that among the two lowest standard deviations of speed-differences between different-model pairs (Figure 25) are those pairs which sampled similarly: 0.94 cm s^{-1} for the VMCM-RCM11 which spread-sample vector averaged over the entire 30 minutes, and 1.12 cm s^{-1} for the SEAGUARD-Aquadopp which burst-sampled in a 1–2 minute vector average interval near the 00 and 30 minute marks. The high-frequency variability during 30 minutes can be estimated by 30-minute high-pass filtering the VMCM data, and that EKE (0.33 to 0.45 cm^2 s^{-2}) is enough to account for about 0.6 cm s^{-1} sampling difference during the 30-minute sampling.

Standard deviation of speed differences for 3 hr low-pass filtered data and with the VMCM rotor stalls excised are shown in Figure 26. The standard deviations are slightly smaller, but the inferences appear to be unchanged.

The random scatter of differences between current speed measurements, summarized in Tables 17 and 18, can be accounted for by the sums of variance:

- differences due to vertical separation (6m–30m) on the mooring (turbulence?): 0.15 to 0.50 cm^2 s^{-2}
- differences due to individual noise-floor estimates for EKE $<$ 3hr in Table 16: 0.33 to 0.45 cm^2 s^{-2}
- differences due to spread versus burst sampling: $\sim$ 0.1 cm^2 s^{-2}

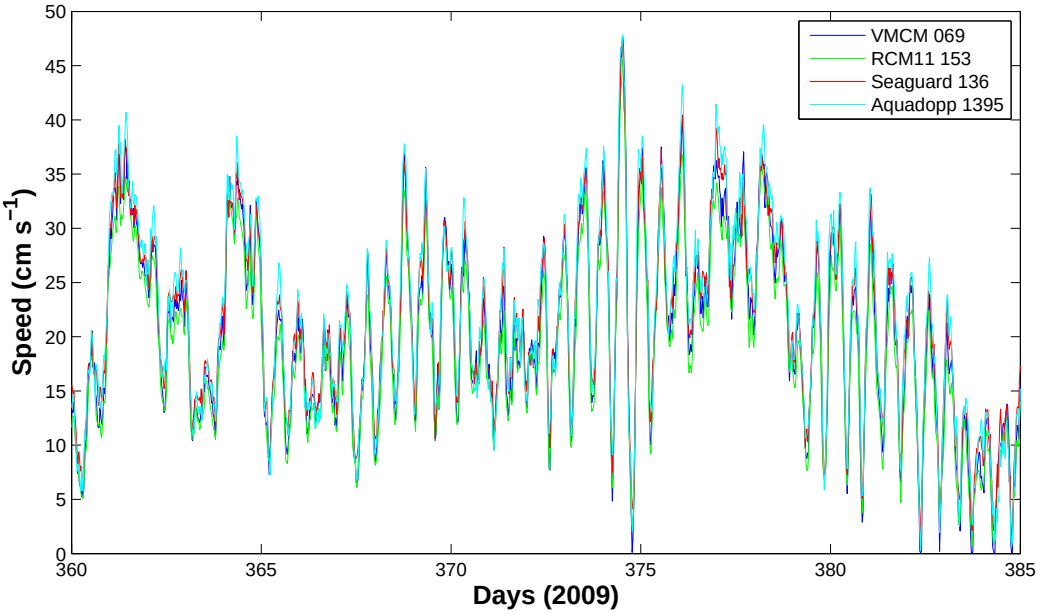

Figure 18: Twenty-five day (360–385) time series of current speed. All records have been corrected for sound speed and tilt and interpolated to a common 30-minute timebase. The VMCM data were 30-minute lowpass filtered.

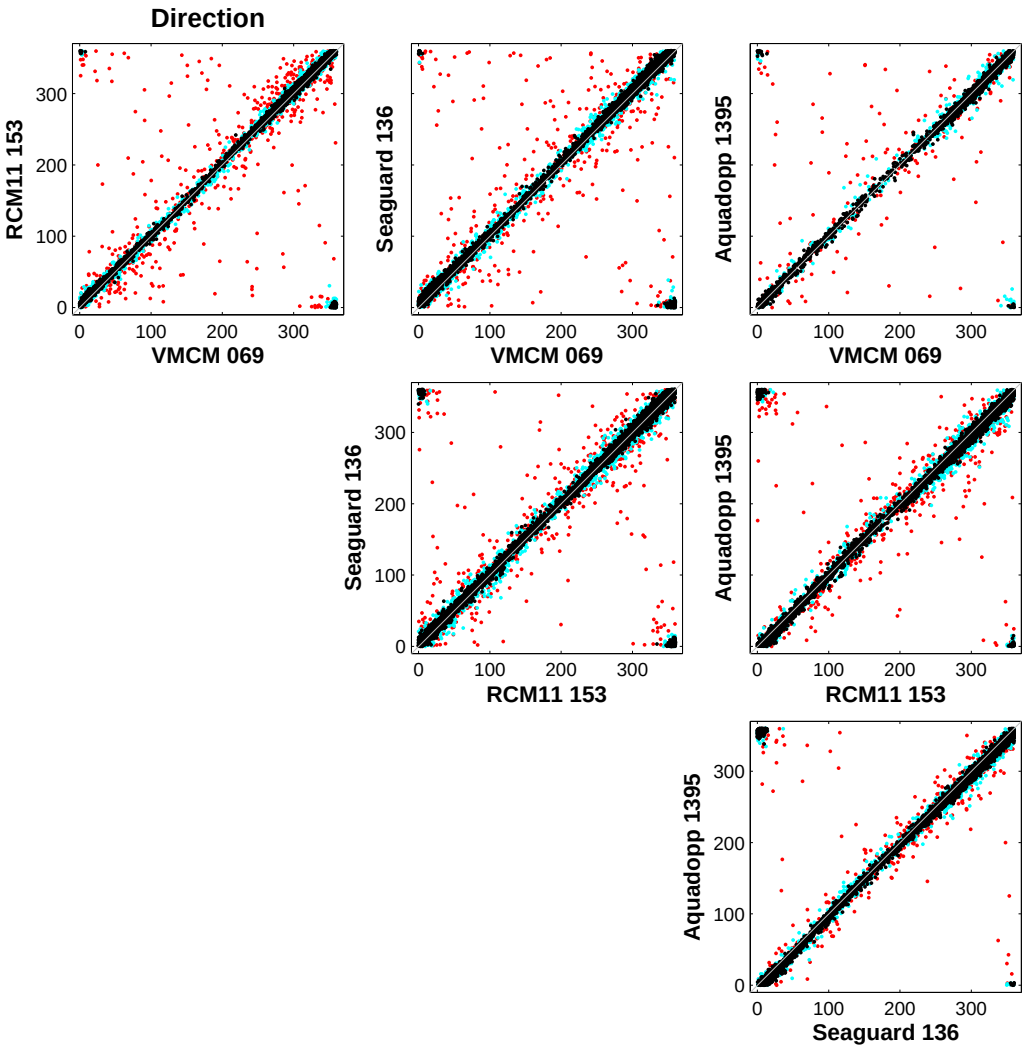

Figure 19: Scatter plots of current direction for different model pairs for all coincident data. All records have been corrected for sound speed and tilt and interpolated to a common 30-minute timebase. The VMCM data were 30-minute lowpass filtered. Red dots correspond to speeds <= 5 cm s^{-1}, cyan to speeds > 5 cm s^{-1} and <10 cm s^{-1}, and black to speeds >=10 cm s^{-1}. Gray line has a slope of one.

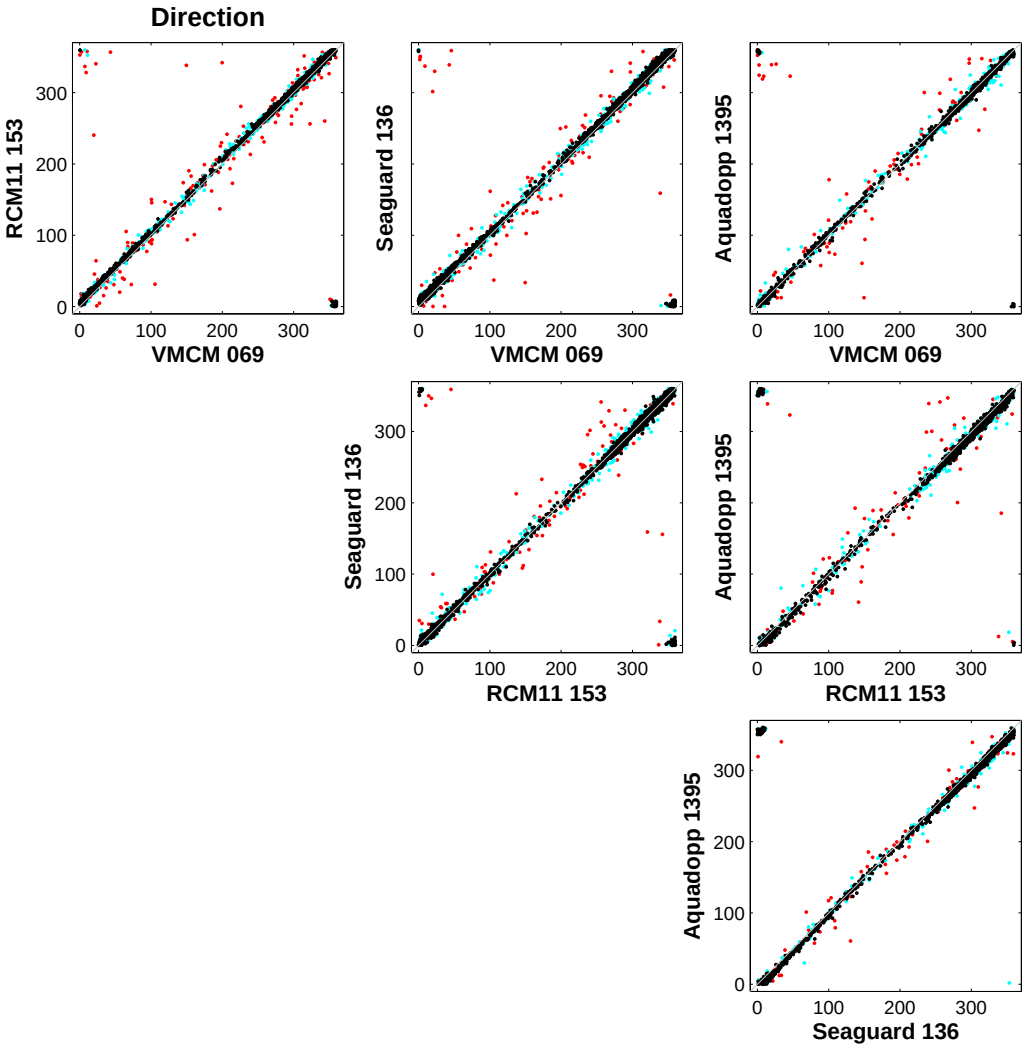

Figure 20: Same as Figure 19 except all records were 3-hour lowpass filtered.

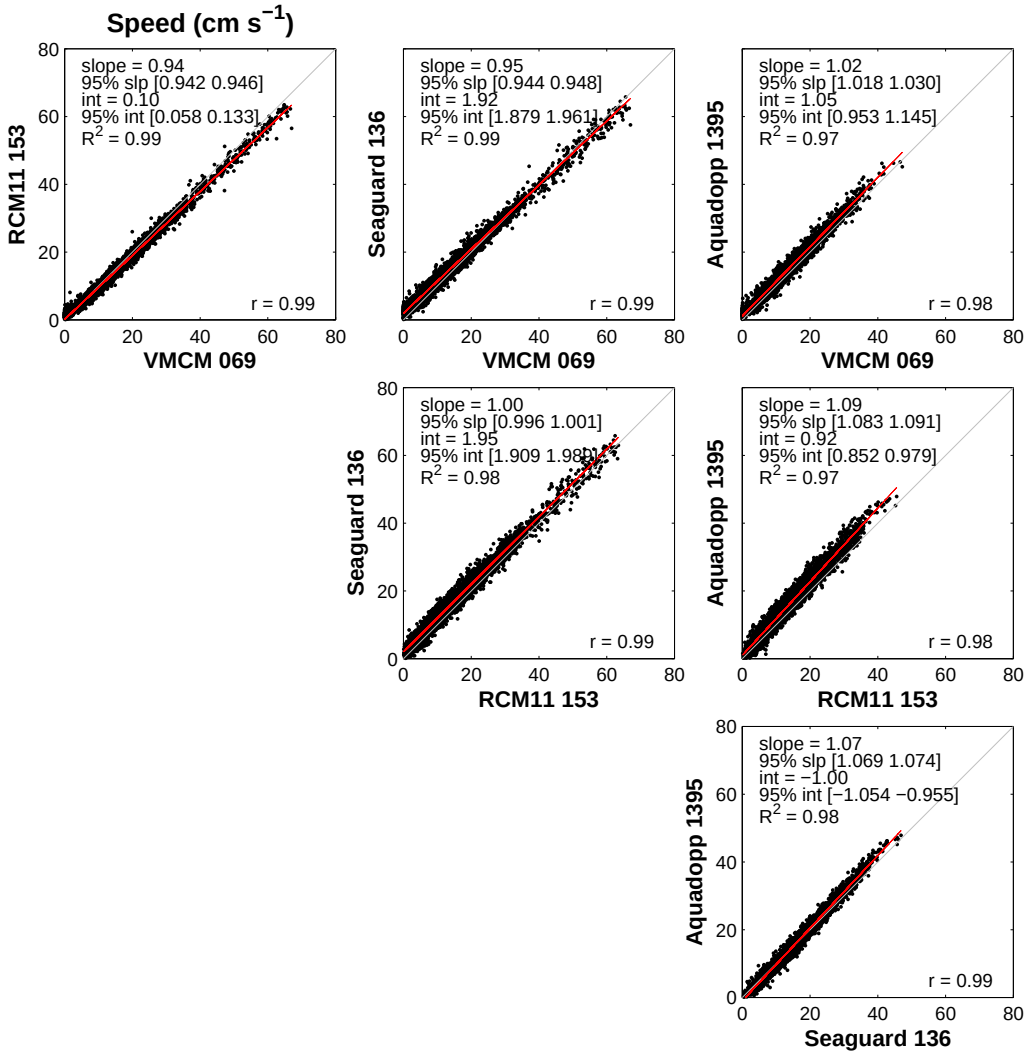

Figure 21: Scatter plots of current speed for different model pairs for all coincident data. All records have been corrected for sound speed and tilt and interpolated to a common 30-minute timebase. The VMCM data were 30-minute lowpass filtered. The gray line has a slope of one. The red line is the fit to the data. The Aquadopp pairings span a lower range of speeds because the Aquadopp stopped before the highest current speed event. The slope and intercept of the red line and their confidence intervals are listed in the upper left corner of each plot.

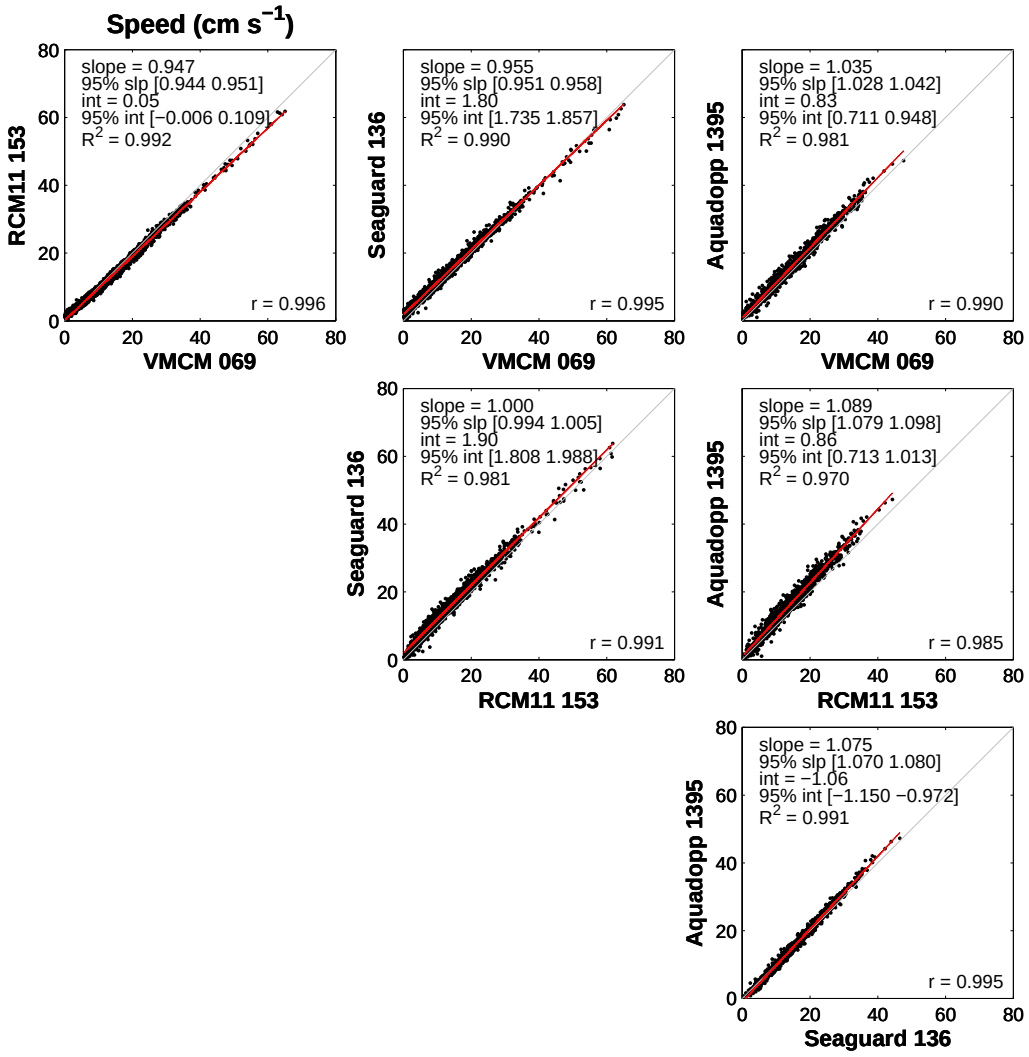

Figure 22: Same as Figure 21 except all records were 3-hour lowpass filtered.

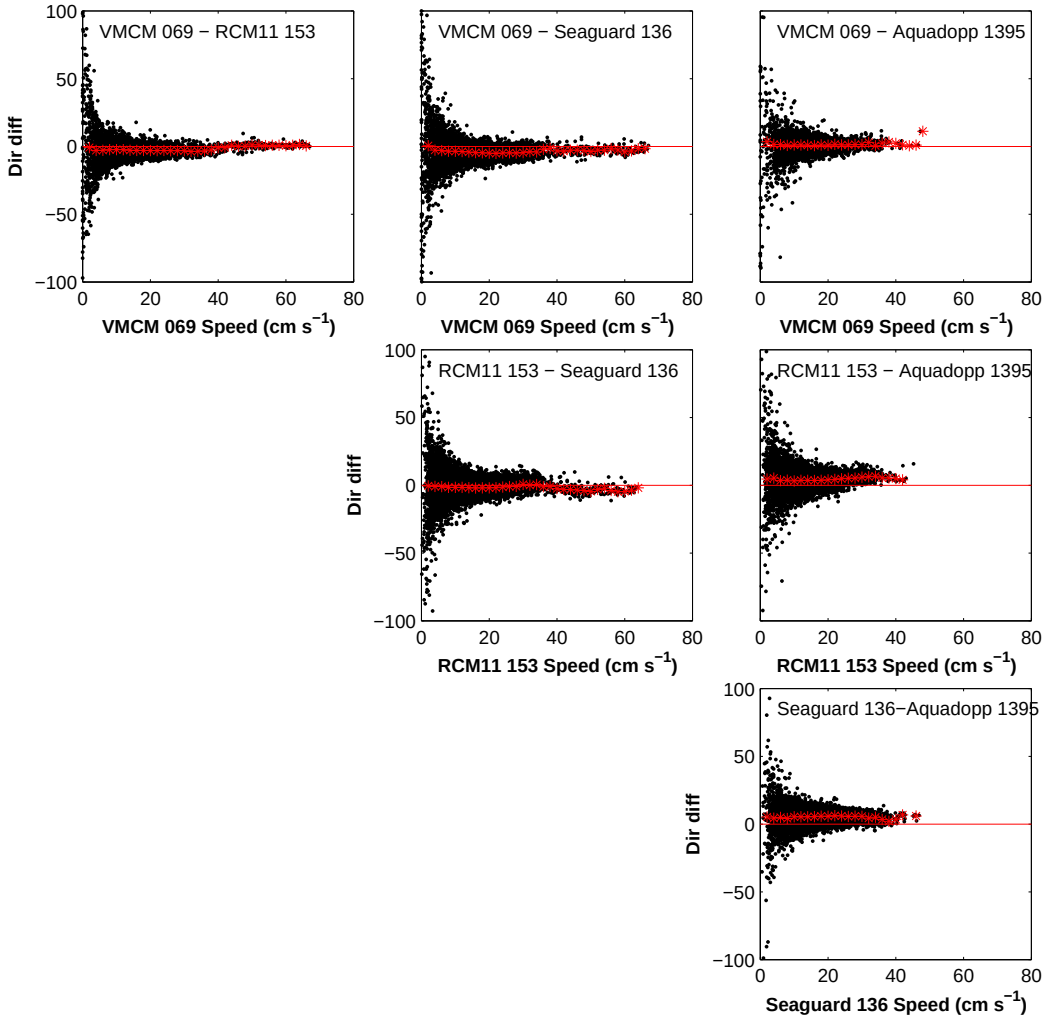

Figure 23: Scatter plots of the difference in current direction versus speed for all coincident data. All records have been corrected for sound speed and tilt and interpolated to a common 30-minute timebase. The VMCM data were 30-minute lowpass filtered. The asterisks represent the median difference calculated for 2 cm s^{-1} bins.

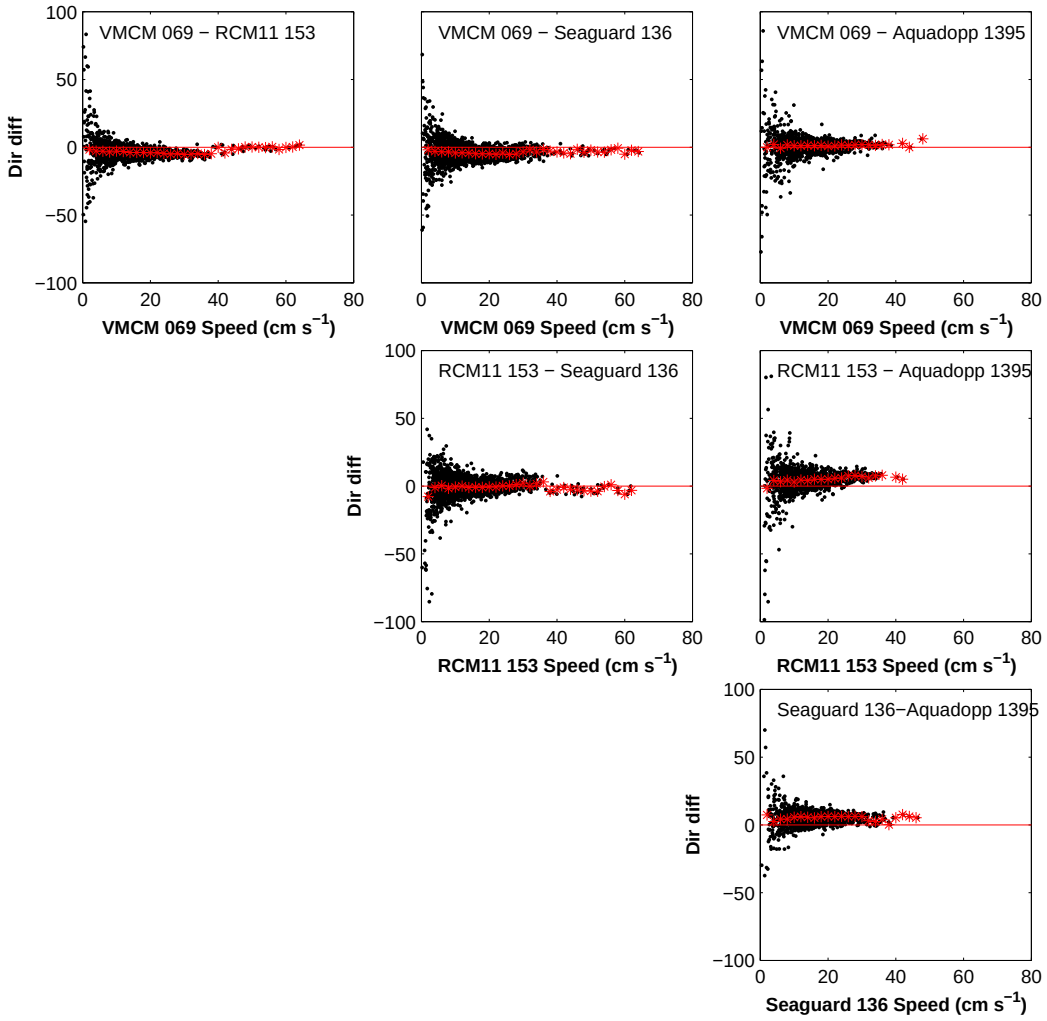

Figure 24: Same as Figure 23 except all records were 3-hour lowpass filtered.

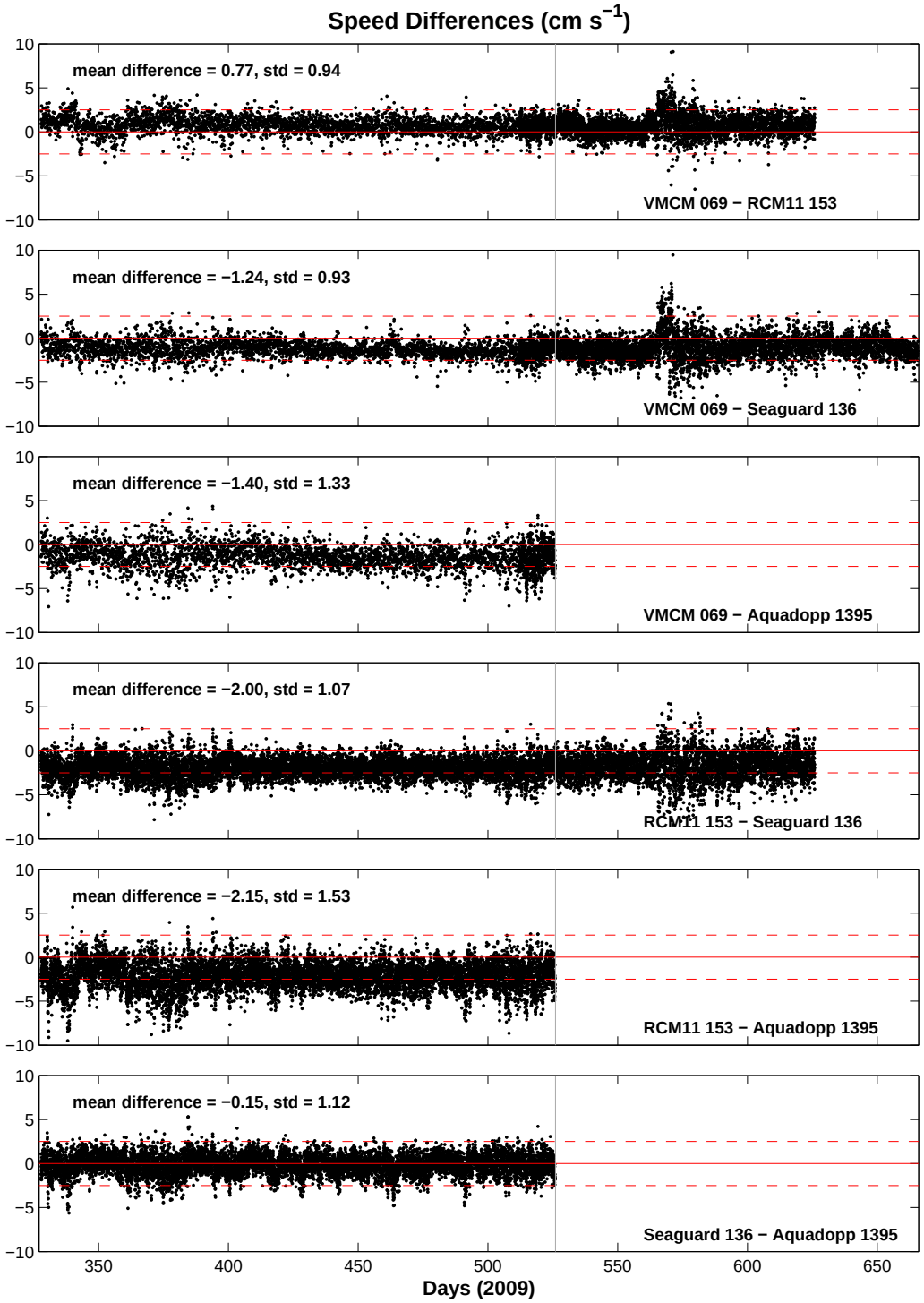

Figure 25: Time series of speed differences between current meters for coincident data. All records have been corrected for sound speed and tilt and interpolated to a common 30-minute timebase. The VMCM data were 30-minute lowpass filtered. The means and standard deviations shown in the plot panels and listed in Table 17 were calculated for the common time period, days 327–525. Day 525 is indicated by the grey vertical line. Solid red indicates the zero line, the dashed red lines indicate ± 2.5 cm s^{-1}.

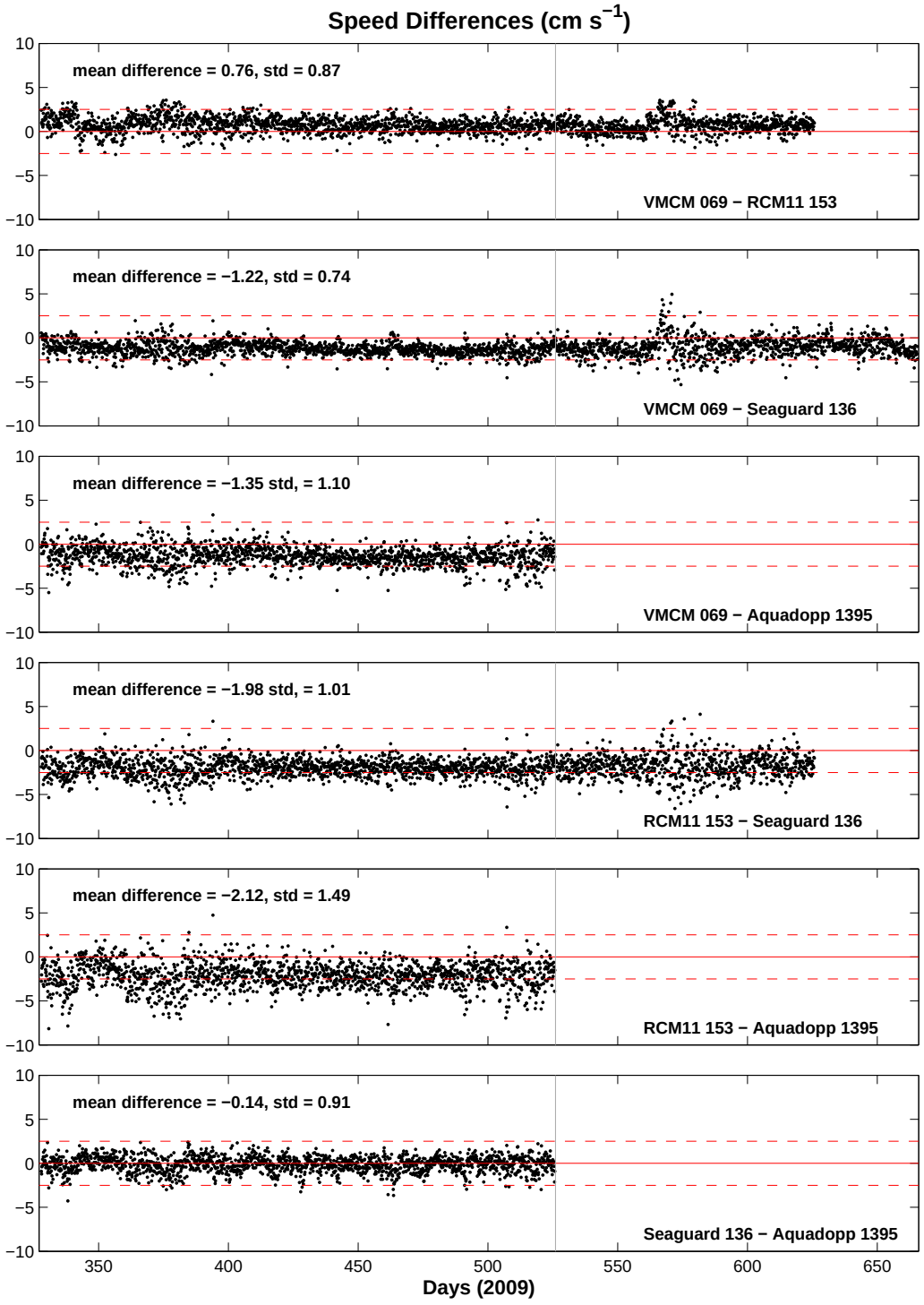

Figure 26: Same as Figure 25 except all records were 3-hour lowpass filtered and means and standard deviations are listed in Table 18

.

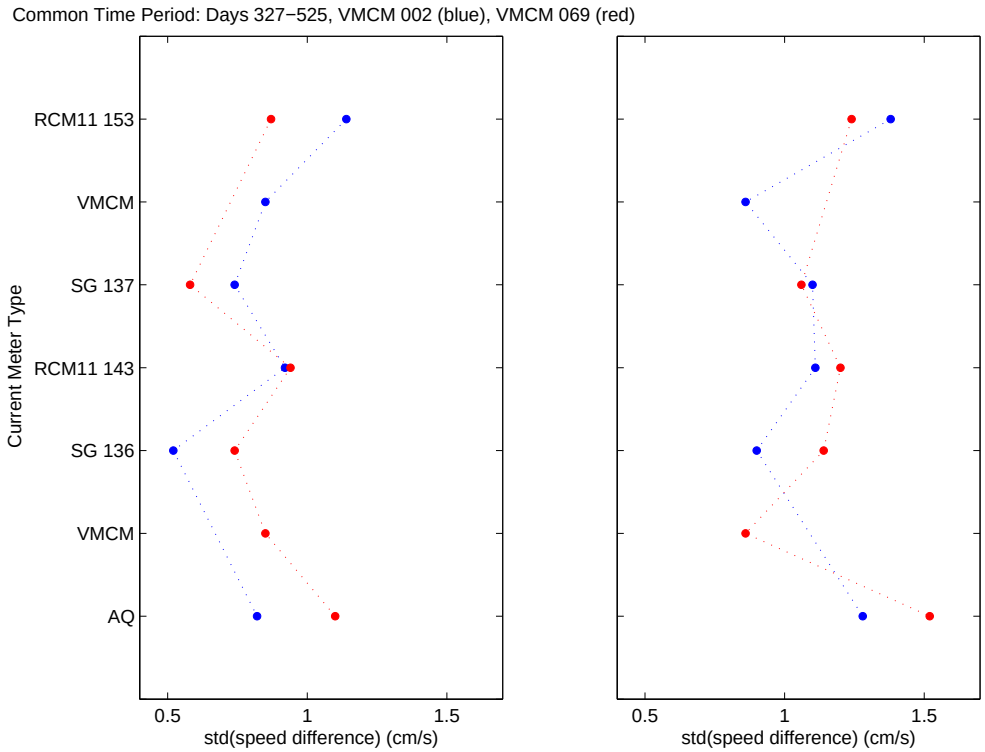

Figure 27: Standard deviation of speed differences between VMCMs and other current meters for the common time period (days 327–525). Left: 3-hr low-pass filtered records. Right: 30-minute intervals from which any VMCM rotor stalled were excised prior to the calculations. The speed differences tend to increase with vertical separation between current meters.

	RCM11 153	VMCM069	SG 137	RCM11 143	SG 136	VMCM002	AQD1395
RCM11 153		-0.77	-1.74	-0.06	-2.00	-0.38	-2.15
VMCM 069	0.94		-0.99	0.69	-1.24	0.43	-1.40
SG 137	0.90	0.72		1.68	-0.26	1.38	-0.41
RCM11 143	0.90	0.96	0.80		-1.94	-0.30	-2.09
SG 136	1.07	0.93	0.79	0.80		1.63	-0.15
VMCM 002	1.24	1.06	0.94	0.89	0.68		-1.79
AQD 1395	1.53	1.33	1.36	1.30	1.12	0.96	

Table 17: Speed difference statistics. Speed differences (upper current meter speed minus deeper current meter speed) in cm s^{-1} were calculated between all pairs. The mean and standard deviation are tabulated respectively in upper right and lower left triangles. The common time period (days 327–525) was used. All records have been corrected for sound speed and tilt and interpolated to a common 30-minute timebase. The VMCM data were 30-minute lowpass filtered.

	RCM11 153	VMCM069	SG 137	RCM11 143	SG 136	VMCM002	AQD1395
RCM11 153		-0.76	-1.69	-0.08	-1.98	-0.34	-2.12
VMCM 069	0.87		-0.93	0.68	-1.22	0.42	-1.35
SG 137	0.81	0.58		1.62	-0.28	1.35	-0.42
RCM11 143	0.77	0.94	0.80		-1.90	-0.26	-2.04
SG 136	1.01	0.74	0.58	0.84		1.64	-0.14
VMCM 002	1.14	0.85	0.44	0.92	0.52		-1.78
AQD 1395	1.49	1.10	1.16	1.31	0.91	0.82	

Table 18: Same as Table 17 except all data were 3-hour lowpass filtered. This reduced the standard deviations, and the means were essentially unchanged.

5.4 Response Function Analyses

As an alternative to regression analyses, response functions were calculated between pairs of current meters using their u and v current components. The window length selected for these analyses was 100 points (50 hours) to smooth the response functions by averaging over many ensemble members. At periods longer than 5 or 10 hours the smoothed admittance magnitudes, $|Admittance|$, reached a plateau, near one (Figures 28-32 and Tables 19-20 which list the average admittance of u and v components for periods longer than 10 hours). We also examined the results from longer windows and longer periods, such as 10 and 40 days (not included here), and verified that the plateau of $|Admittance|$ extended to those longer periods.

This analysis was first performed on the three same-model pairs for the common time period (Figure 28). Their speed records were already known to be nearly identical, and we wanted to examine at what higher range of frequencies the response functions differed significantly from unity. For this analysis VMCM 002 direction was rotated 8 degrees to the left and then speed and direction were converted back to u and v. At periods shorter than 5 days, the response magnitudes fall off rapidly to 0.2. We interpret that drop as a signature of real differences in the turbulent currents between their nearby locations on the mooring. The phase becomes noisy when the response magnitude drops.

Using the same procedure, we performed response analyses on different-model pairs for both the common time period and the first high-speed event. (The first high-speed event lasted 21 days and provided enough averaging of 50-hour ensemble members, but the later highest-speed event only lasted 7 days, which was too short to produce smooth response functions.) In these cases (Figures 29 - 32) the admittance magnitudes ($|Admittance|$) reached plateaus further from unity than same-model pairs for long periods ($<$5 to 10 days, as above) indicating a current speed bias between the instruments. For the high-speed event we were particularly interested to check whether the plateau heights remained the same as for the weaker currents during the common time period. While they are bumpier due to less averaging, the levels stay about the same, as listed for both intervals in Table 20.

The response admittance magnitudes basically agree with the results of speed-ratios, and all these measures of relative current measurements are summarized in Table 22 and discussed in the Summary.

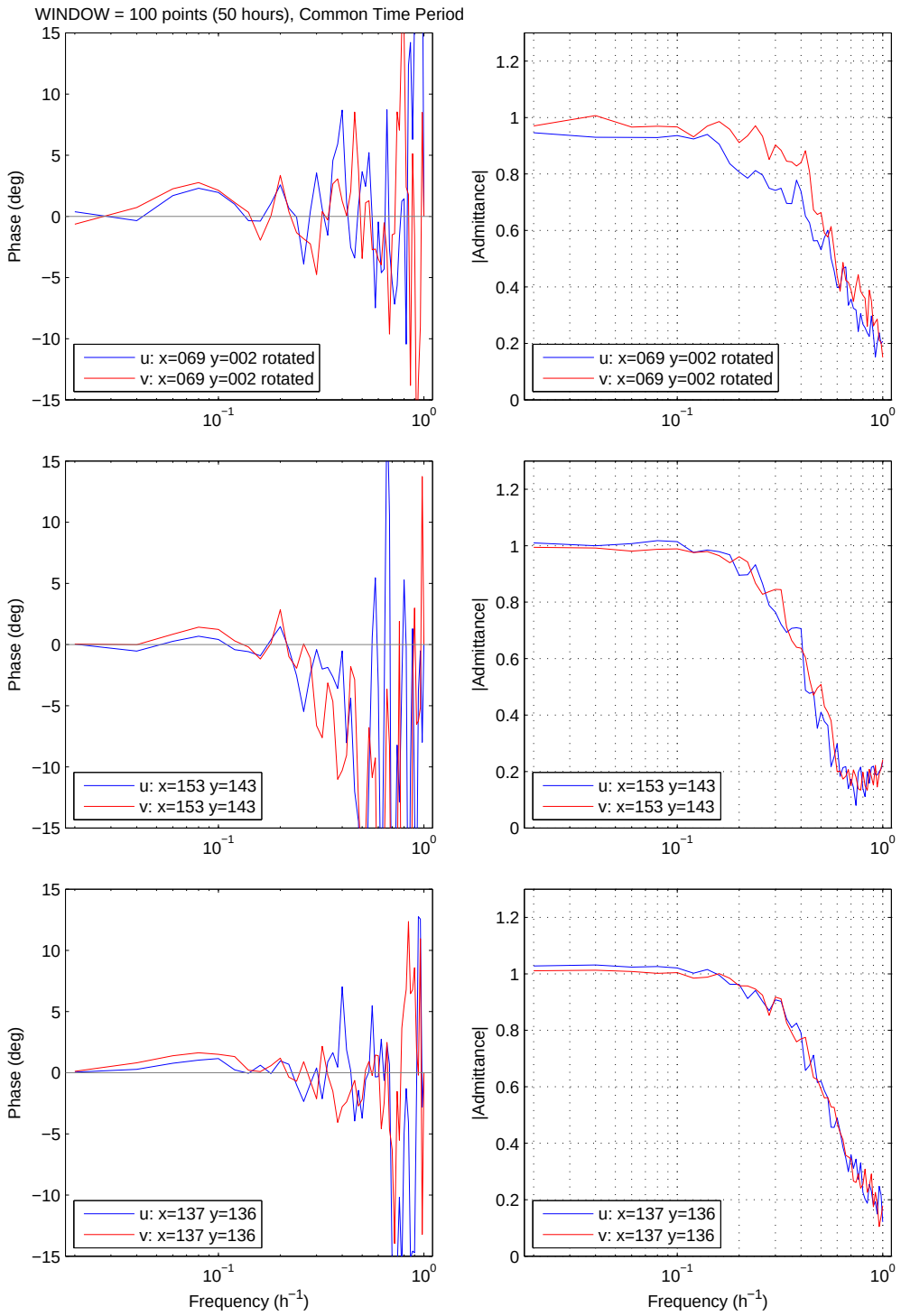

Figure 28: Phase (left) and Admittance (right) for same-model pair u and v components. VMCM 002 direction was rotated 8 degrees to the left and converted back to u and v. Top: VMCM, Middle: RCM 11, and Bottom: SEAGUARD.

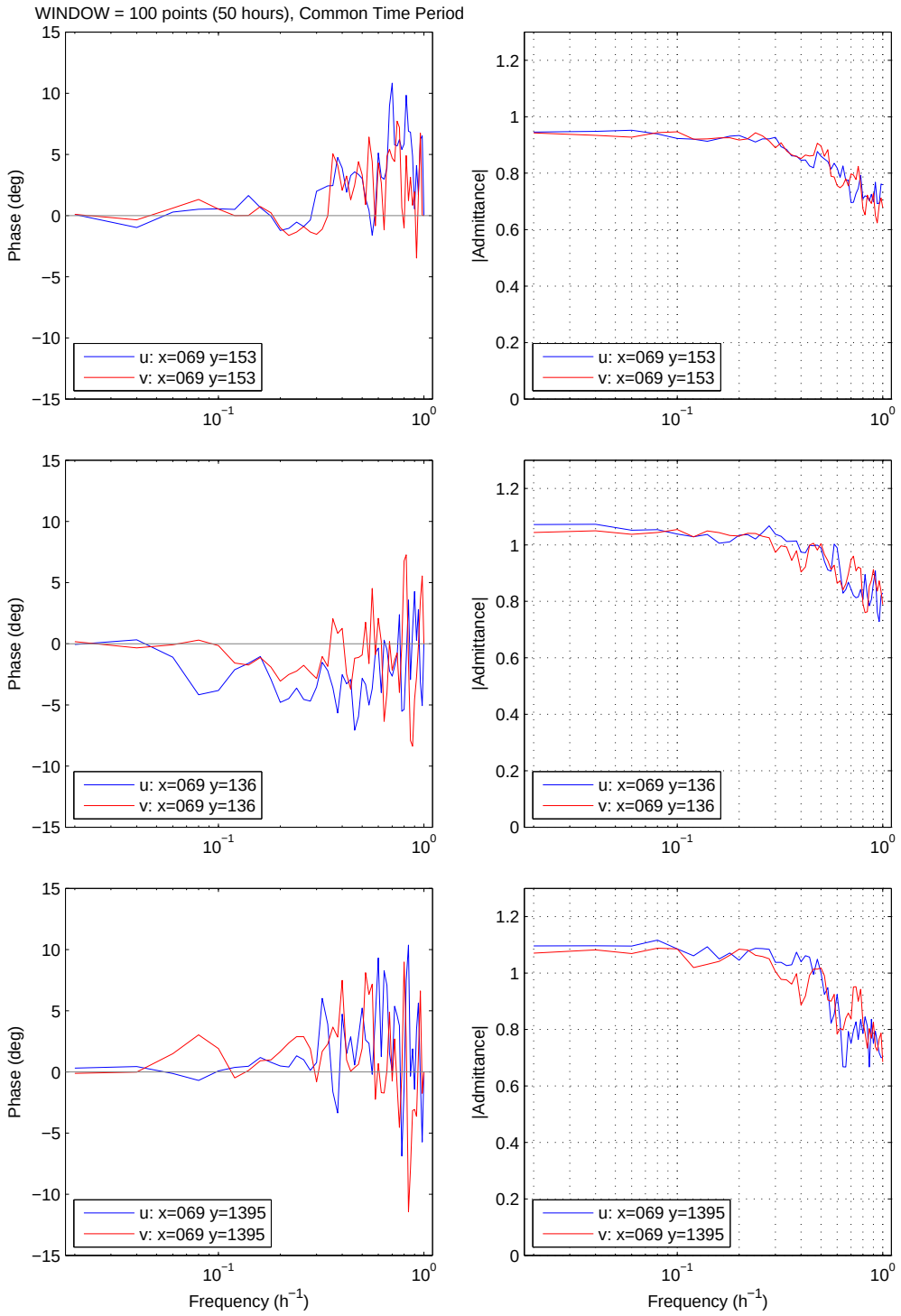

Figure 29: Phase (left) and Admittance (right) for different-model pair u and v components for the common time interval. VMCM 069 is compared to: RCM11 153 (top), SG 136 (middle) , and Aquadopp (bottom).

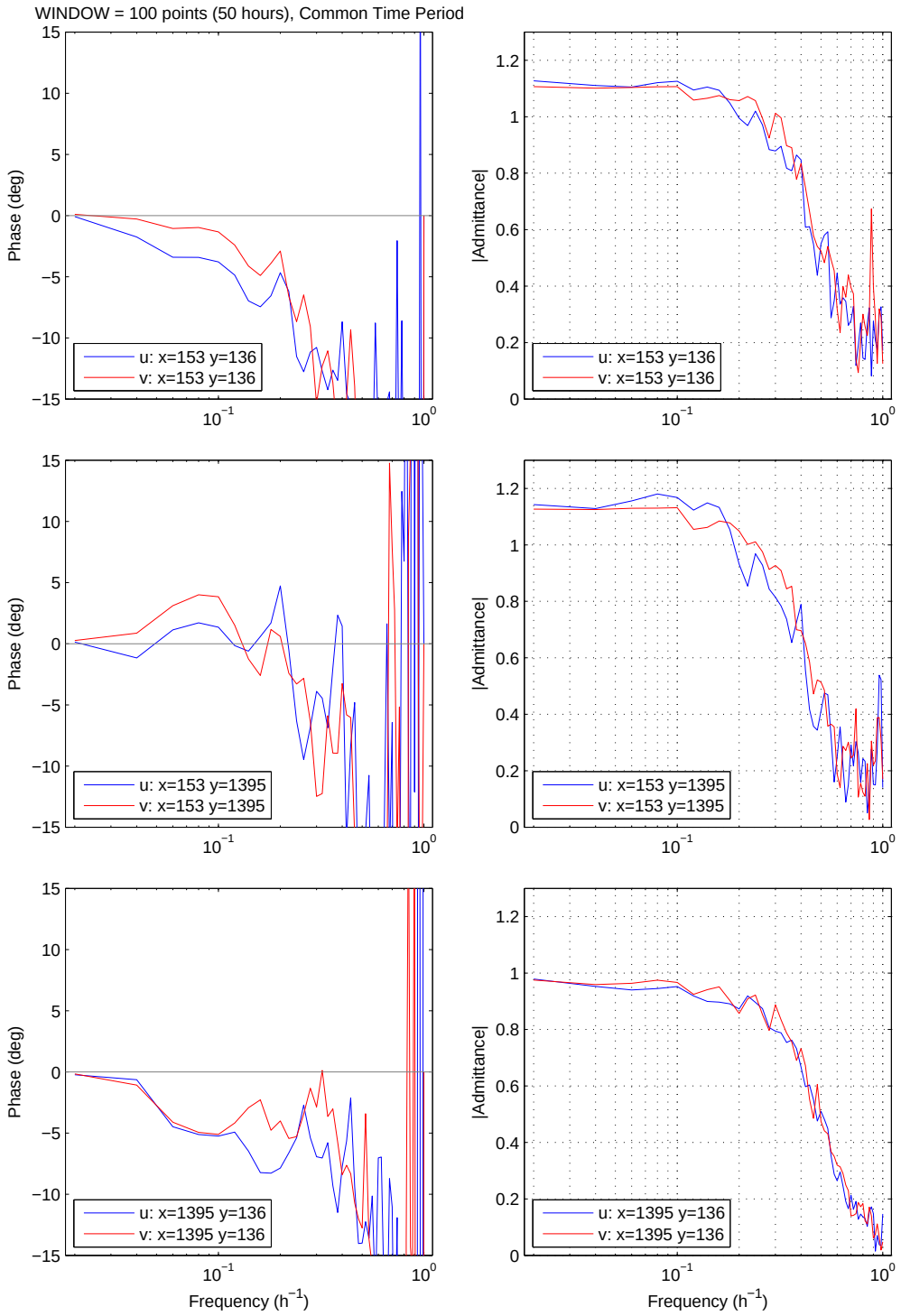

Figure 30: Phase (left) and Admittance (right) for different-model pair u and v components for the common time interval. RCM11 153 versus SG 136 (top), RCM 11 153 versus Aquadopp (middle), and Aquadopp versus SG 136 (bottom).

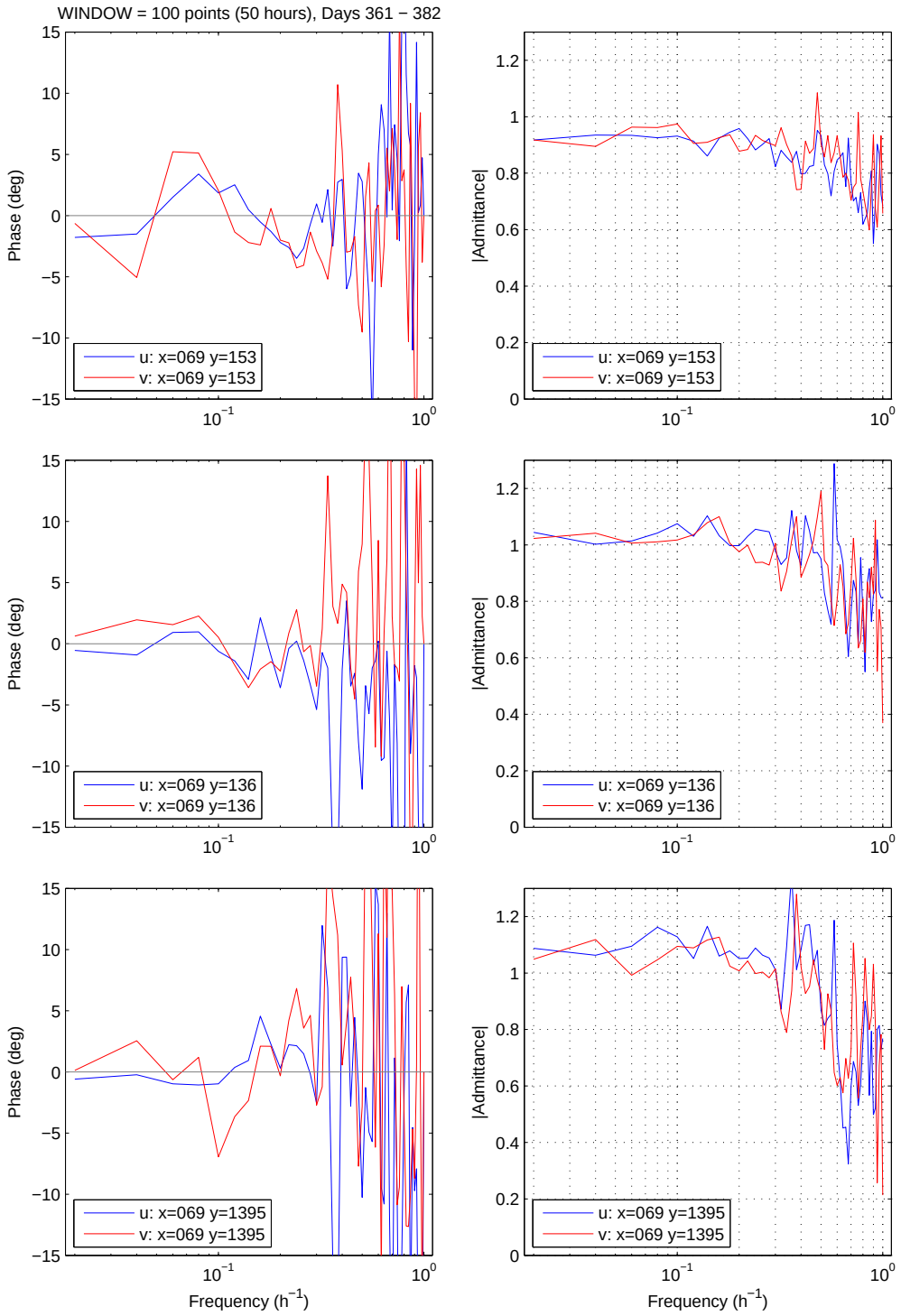

Figure 31: Phase (left) and Admittance (right) for different-model pair u and v components for the first high speed event (days 361–382). VMCM 069 is compared to: RCM11 153 (top), SG 136 (middle) , and Aquadopp (bottom).

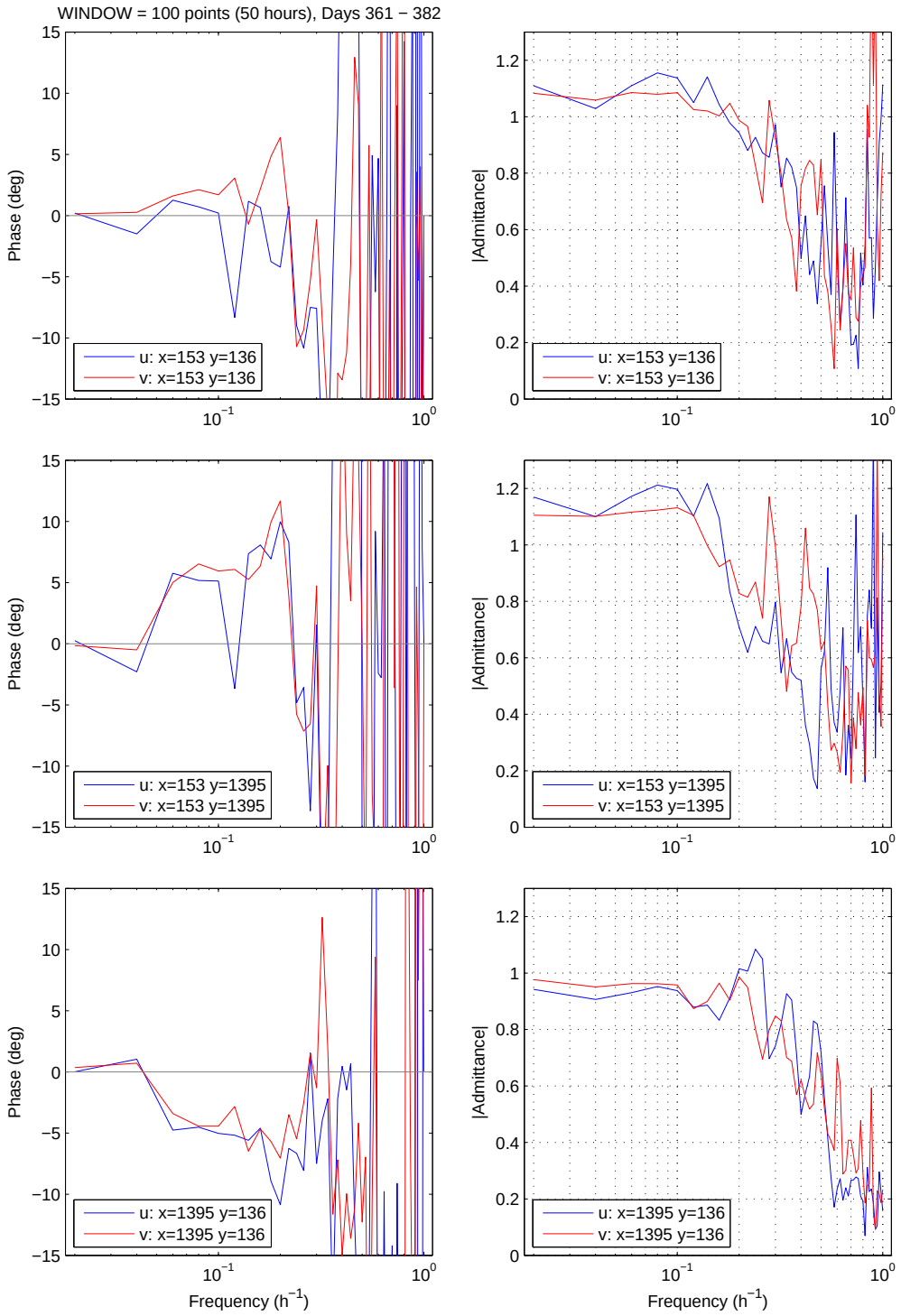

Figure 32: Phase (left) and Admittance (right) for different-model pair u and v components for the first high speed event (days 361–382). RCM11 153 versus SG 136 (top), RCM 11 153 versus Aquadopp (middle), and Aquadopp versus SG 136 (bottom).

Current Meter Pair	Admittance
VMCM 069/002	0.96
RCM11 153/143	1.00
SG 137/136	1.02

Table 19: Same-model low-frequency admittance for u and v components. Each pair of numbers represents the common time interval (days 327–525).

	RCM11 153	SG 136	AQD1395
VMCM 069	0.93 | 0.92	1.04 | 1.03	1.07 | 1.08
RCM11 153		1.11 | 1.08	1.14| 1.12
AQD 1395		0.96 | 0.96	

Table 20: Different-model low-frequency admittance for u and v components. Each pair of numbers represents the common time interval (days 327–525) | first high speed event (days 361–382).

5.5 Principal Component Analyses

Principal component analyses were carried out for two time periods: the common time interval (days 327–525) and the highest speed event (days 565-573) using the matlab function princomp. Table 21 lists the percent variance explained by the first three modes for the two time periods.

The mean and mode vectors are plotted as a function of depth level for the common time interval in Figure 33. Note VMCM SN 002 at level 6 appears anomalous and further reinforces the decision to use VMCM SN 069 for inter-comparison purposes. Mode time series are plotted in two different ways: amplitude and phase for modes one and two in Figure 34 and real (u) and imaginary (v) components in Figure 35.

The above figure sequence is repeated in Figures 36-38 for the highest speed event.

Mode	Common Time Period Days 327–525	Highest Speed Event Days 565–572
1	99.4	98.8
2	0.2	0.8
3	0.2	0.2

Table 21: Percent variance explained from principal component analyses.

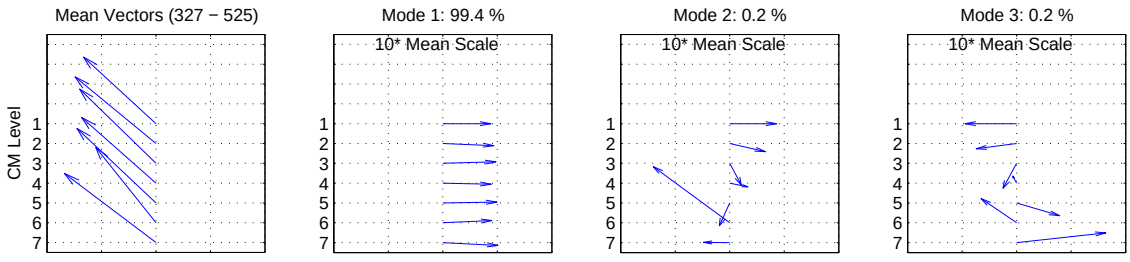

Figure 33: Mean (left) and mode vectors (panels 2–4) for common time period (days 327–525) as a function of current meter depth level. See Table 1 for level information.

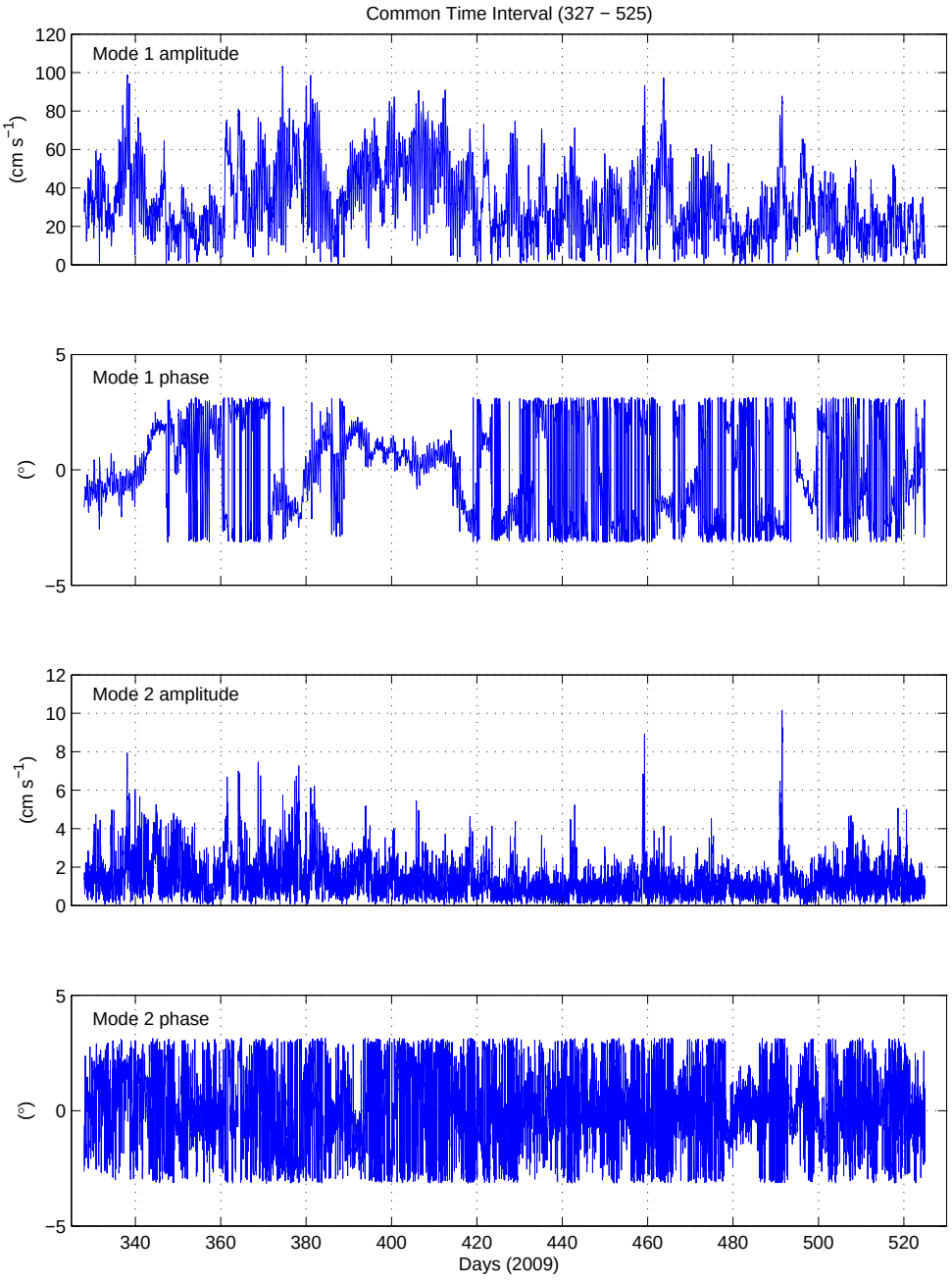

Figure 34: Time series of amplitude for modes one (panel 1) and two (panel 3) for the common time period (days 327–525), phase is shown in panels 2 (mode 1) and 4 (mode 2).

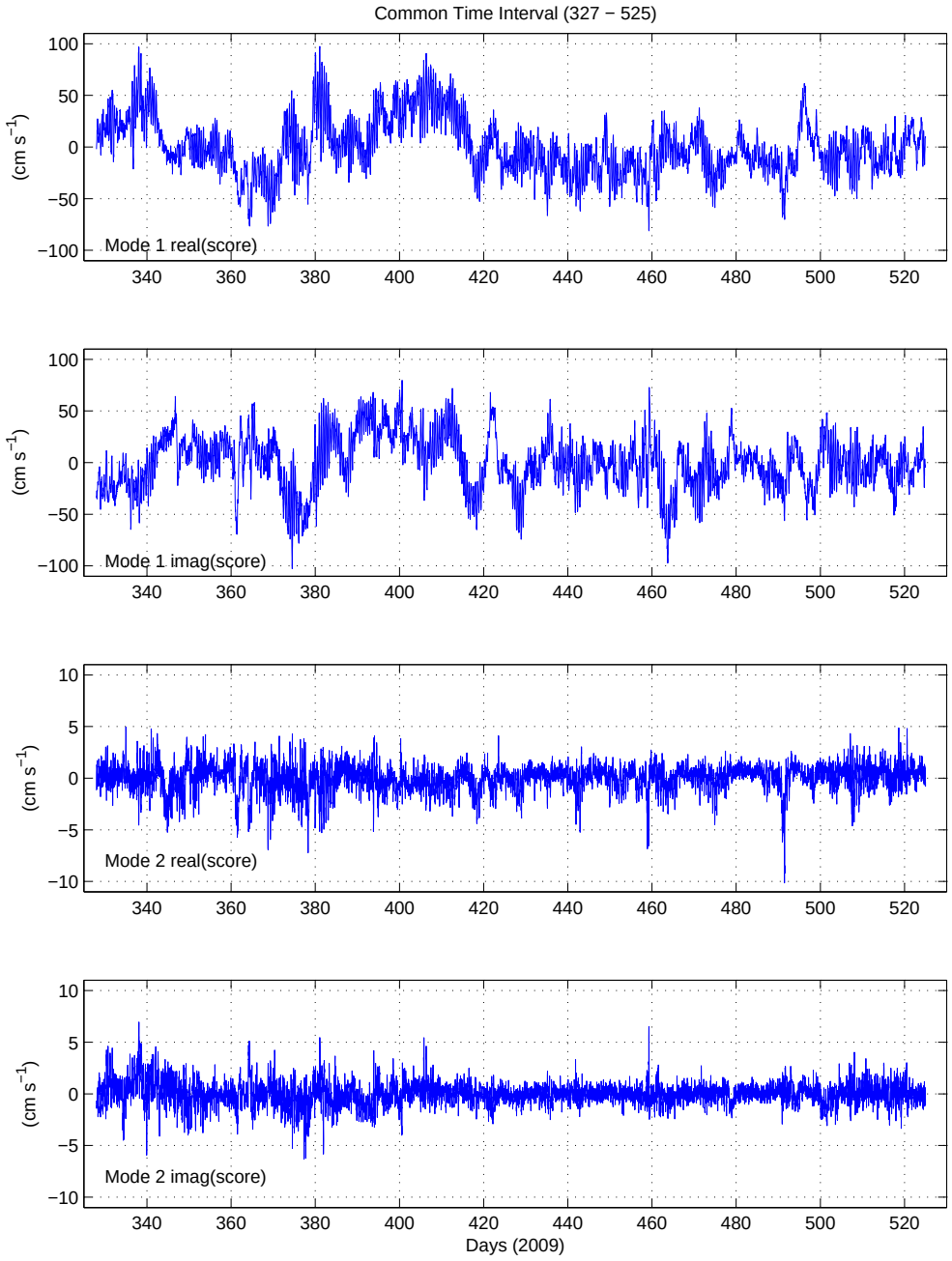

Figure 35: Real time series (u) for modes one (panel 1) and two (panel 3) for the common time period (days 327–525), the imaginary time series (v) is shown in panels 2 (mode 1) and 4 (mode 2).

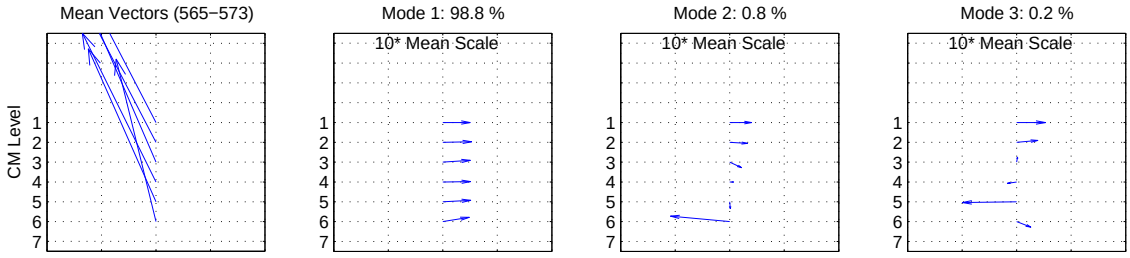

Figure 36: Mean (left) and mode vectors (panels 2–4) for highest speed event (days 565–573) as a function of current meter depth level. The Aquadopp (level 7) had stopped by this time. See Table 1 for level information.

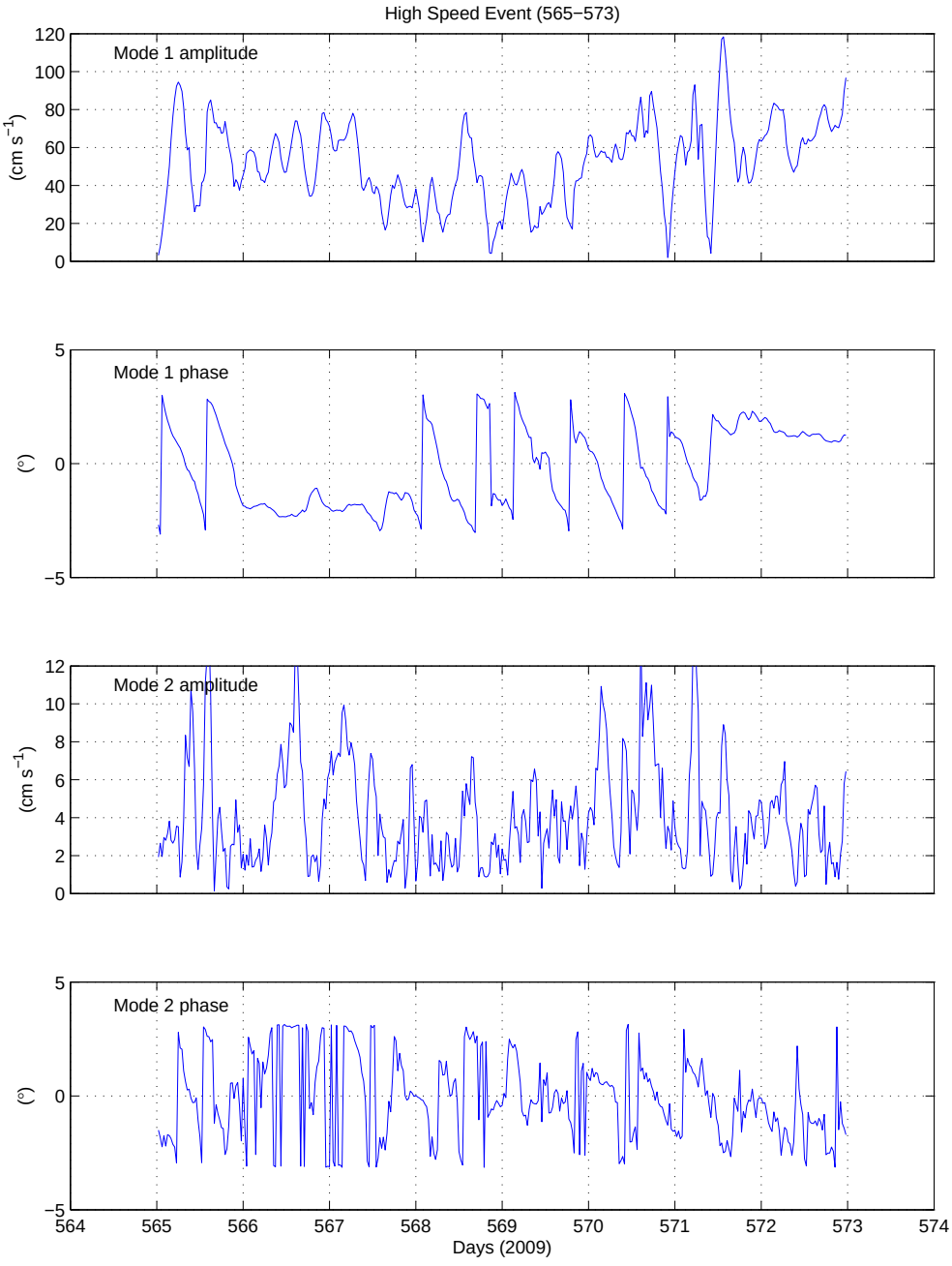

Figure 37: Time series of amplitude for modes one (panel 1) and two (panel 3) for the highest speed event (days 565–573), phase is shown in panels 2 (mode 1) and 4 (mode 2).

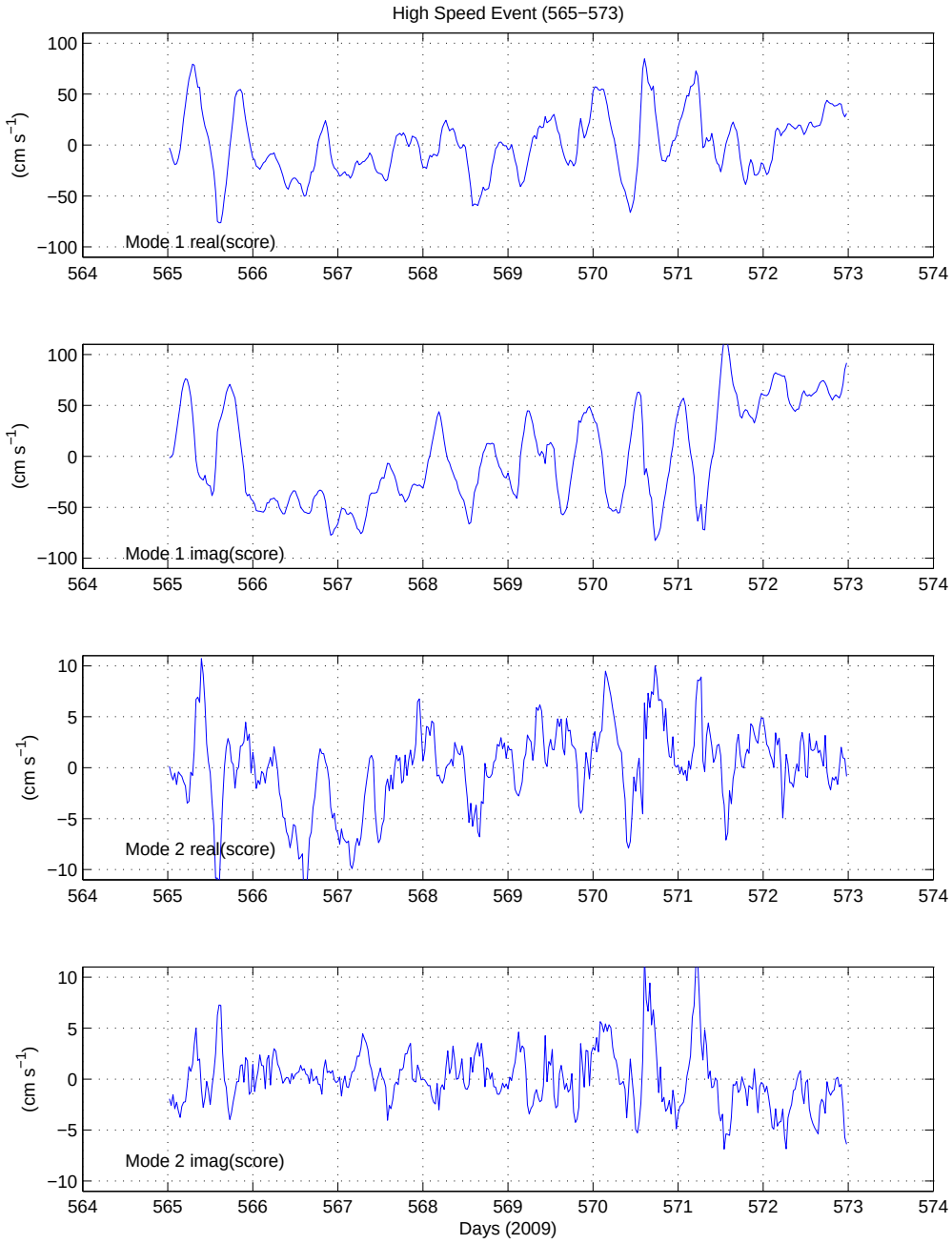

Figure 38: Real time series (u) for modes one (panel 1) and two (panel 3) for the highest speed event (days 565–573), the imaginary time series (v) is shown in panels 2 (mode 1) and 4 (mode 2).

6 Summary

Current-speed measurements in general agreed well among all the instruments. Two types of same time-interval comparisons were conducted:

1. Current speeds after vector-averaging over three separate time-intervals:
   (a) a 198-day common time interval,
   (b) a 21-day high-speed event, and
   (c) a 7-day highest-speed event;
2. current-speed measurements at 30-minute sampling intervals:
   (a) calculating the slopes of xy scatter-plots,
   (b) calculating the means of their speed-difference time series, and
   (c) calculating the average admittance magnitude for u and v components.

Item 2b is sensitive to how each sample is taken and whether it is spread-sampled or burst-sampled within each 30-minute sampling interval. It accounts for the width of the scatter-plots in method 2a.

The findings from comparisons (1a,b,c and 2a and c) are summarized in Table 22. The low frequency and mean findings (1a, b, c and 2c) are summarized in its right hand column.

The three pairs of same-model current meters have consistent vector-averaged speeds within 1%, and the departures are insignificant within model-type. The VMCMs are at the median vector magnitude speed for all three time-intervals and speed-range measurements. These median measurements of the currents are used for subsequent inter-model comparisons.

The RCM11s produced vector-mean speeds that were about 5% low in low-speed ranges (average 9 and 15 cm s^{-1} for 198 d and 21 d) and agreed with the median VMCM records within 2% for the highest-speed event, which had average currents greater than 35 cm s^{-1} averaged over 7 days. Consequently, while one may choose to increase the RCM11 speeds by 5% in the lower ranges, it is not appropriate to do so for the high range. The summary low frequency speed-correction ratio (and its uncertainty) for RCM11s is 1.04 ($-0.02/+0.03$).

The SEAGUARDS produced vector-mean speeds that were 0% to 5% higher than the median (VMCM) records in the different speed ranges. The slope of the scatter plot against the VMCM indicates the bias (if any) decreases with increasing speed. The summary low frequency speed-correction ratio (and its uncertainty) for SEAGUARDs is 0.97 ($-0.02/+0.03$).

The Aquadopp produced vector-mean speeds that were about 7% higher than the median (VMCM) records in both the common time interval and in the first high-speed event. (Recall its battery had drained before the highest-speed event.) Because its fitted line on

the scatter plot is about 1 cm s^{-1} above and nearly parallel to the 1:1 line, and trending to aproach it with increasing speeds, this amount of overestimate would decrease at higher speeds. Consequently, one might not want to apply a factor of 0.93 to Aquadopp currents at the higher ranges. This reasoning led to our summary speed-correction ratio (and its uncertainty) for the Aquadopp of 0.93 ($-0.02/+0.02$). Supporting these findings, Houk and Johns (unpublished manuscript) found the Aquadopp tended to read anywhere from 0.5 to 2.5 cm s^{-1} higher than the DVS and SEAGUARD and that the speed difference tended to increase proportionally to the absolute current speed.

Current direction measurements improved in agreement between instruments with increasing current speed. At speeds below 5 cm s^{-1}, there was a great deal of scatter in angle whether comparing same-model or different-model current meters. Current angle measurements have $\sim$15 degrees standard deviation, decreasing to $\sim$5 degrees standard deviation at 10 cm s^{-1} speeds, and smaller yet ($\sim$2 degrees) for speeds above 20 cm s^{-1}. Vector-averaged current direction over the common time period showed good agreement with the median direction within $\pm$3 degrees, consistent with manufacturer-specifications, with two exceptions: The compass of VMCM 002 appears faulty with 8 degree offset to the right, and the Aquadopp had 6 degree offset to the left of the median of the others. Houk and Johns (unpublished manuscript) also found the Aquadopp had a slight offset of about -2 to -4 degrees relative to the DVS and SEAGUARD.

The shape and magnitude of these direction-differences versus speed dot-plots can be explained as resulting from a standard deviation in each of the two orthogonal measurements of current vector components of $\delta u_1 \sim 1$ cm s^{-1}. By simple propagation-of-error we estimate

$$\delta\theta \sim \sqrt{2}\,\frac{\delta u_1}{U} \cdot \frac{180}{\pi}$$

expressed in degrees for a single current meter. For two current meters measuring components independently, the difference $\delta u_{\text{diff}} \sim \sqrt{2}\,\delta u_1$ so

$$\delta\theta_{\text{diff}} \sim 2\,\frac{\delta u_1}{U} \cdot \frac{180}{\pi}$$

Because this estimate works well, we do not have to speculate that the ocean currents or the mooring are introducing any added angle variation at low current speeds.

Same-model consistency						
	vector-averaging intervals					
Model	days 327–525 common interval	days 361–382 1st high speed event	days 565–572 highest speed event	$(\text{slope})^{-1}$ of speed scatter plot	Adm^{-1} days 327–525	speed same-model consistency
Source	Table 12	Table 13	Table 14	Figure 12	Table 19	
VMCM SN069/002	9.01/8.82 = 1.02	15.20/14.66 = 1.04	36.64/37.35 = 0.98	1/1.01 =.99	1/0.96 =1.04	1% same as median
RCM11 SN153/143	8.61/8.62 = 1.00	14.39/14.39 = 1.00	34.96/35.77 = 0.98	1/0.98 =1.02	1/1 =1.00	1%
SEAGUARD SN137/136	9.40/9.54 = 0.99	14.91/15.79 = 0.94	35.73/36.17 = 0.99	1/0.98 =1.02	1/1.02 =0.98	1%
Different-model comparisons VMCM is found same as median, so compare other models to median (VMCM069)						
	vector-averaging intervals					
Model	days 327–525 common interval	days 361–382 1st high speed event	days 565–572 highest speed event	$(\text{slope})^{-1}$ of speed scatter plot	Adm^{-1} days 327–525	summary speed-correction ratio
Source	Table 12	Table 13	Table 14	Figure 21	Table 20	
ratio (median/model-type)				vs. VMCM069		
RCM11	9.01/8.62 =1.05	14.91/14.39 =1.04	35.97/35.37 =1.02	1 / 0.94 = 1.06	1/0.93 =1.07	1.04 -0.02/+0.03
SEAGUARD	9.01/9.47 =0.95	14.91/15.35 =0.97	35.97/35.95 =1.00	1 / 0.95 = 1.05	1/1.04 =0.96	0.97 -0.02/+0.03
Aquadopp	9.01/9.73 =0.93	14.91/16.11 =0.93	NA	1 / 1.02 = 0.98	1/1.07 =0.93	0.93 -0.02/+0.02

Table 22: Current magnitude measurements summary. For different-model comparisons, the sense of each entry is the multiplication factor which would make that current meter agree best with the median (VMCM). Hence the inverse slope and inverse admittance are listed. The rows labeled RCM11 and SEAGUARD summarize the instrument-pair analyses except for columns 5 and 6 where the slope and response function analysis are presented for only RCM 153 in row labeled RCM11 and SEAGUARD 136 in row labeled SEAGUARD.

7 Acknowledgments

We gratefully acknowledge the crew of *R/VIB Nathaniel B. Palmer* and the team of technicians from the Raytheon Polar Sciences group for their willing and competent efforts during the deployment and recovery cruises. Erran Sousa at URI deserves particular acknowledgment for successful recovery of the mooring, reestablishing acoustic transponding with it after a worrisome interval of several hours when all communication had been lost while it rose to the surface in thick fog conditions. At WHOI we wish to thank Rick Trask and Ruthanne Molineaux and the Rigging Shop for mooring preparation, Scott Worrilow and Sean Patrick Whelan for instrument preparation, Nan Galbraith for reading the binary VMCM files and converting them to MATLAB, and Bob Weller and Geoff Allsup for advise regarding the VMCMs. At AADI we wish to thank Brandon Reiff, Ivan Victoria, Richard Butler, and Anders Tengberg. At Nortek we wish to thank Malcolm Williams, Eric Siegel, and Atle Lohrmann. We thank Adam Houk and William Johns at the University of Miami for sharing the results of their current meter intercomparison. We thank Mark Wimbush for helpful discussions regarding the data records. This work was supported by the U.S. National Science Foundation, Grant ANT-0635437.

A Checking for non-dependence of height off bottom

We seek in this appendix to characterize whether speed and angle differences depend solely upon different instrument models, or whether they might depend partly upon height off the bottom in a benthic boundary layer/ bottom Ekman layer. We examine the means and standard deviations of the currents and examine nearby CTD profiles for evidence of bottom mixed-layer thickness.

Over a smooth bottom like at this mooring site, the theoretical boundary-layer thickness would be proportional to the current speed U 'at infinity', with $H_{ml} \sim \kappa u^*/f$ and $u^* \sim U/30$, which works out to 67 m for $U = 0.6$ m s^{-1} and von Karman's coefficient $\kappa = 0.4$ and $f = 1.2e^{-4}$ sec^{-1} at 57°S. This is a steady-state theory, whereas the currents had semidiurnal fluctuations of at least half the amplitude during the observed high-current events. So the theory is only a rough guideline. Over a rough bottom the thickness can be greater. The concern here is to provide evidence that mooring heights 100 m off bottom are comfortably above the Ekman and mixed-layer height. In highest currents and tilts, the mooring pulled down nearly 40 m, so the lowest current meter would be 60–70 m off bottom. Thus, partly because of the lost buoyancy from two broken glass floats, the lowest current meters would not assuredly remain always above the boundary layer, and this section investigates this question.

Figure 39 shows the mean speeds and angles plotted versus height off the bottom. The means for the common time period, and for the highest-speed event are shown, because the mooring pulls down 20 m to a maximum of 40 m in high currents. Moreover, the theoretical thickness of a benthic boundary layer increases with current speed. So high-speed events would be more likely to exhibit height dependence if it can be seen at all.

In a bottom Ekman layer in the southern hemisphere the angles relative to the velocity outside the Ekman layer would veer to the right and the speeds would be expected to decay approaching the bottom. This is not what was observed in any of the panels and time intervals, but instead the mean speed and angle differences between depths are mainly associated with model type rather than upon height off the bottom (Figure 39). In the highest speed event there is instead a hint of bottom-intensification. This may resemble the bottom-intensification observed in eddies under the Kuroshio Extension by *Bishop et al.* [2011], however in this case the limited vertical separation (~ 30 m) of these measurements would poorly estimate vertical trapping scales of 3 to 11 km.

On each of the deployment and recovery cruises CTDs were taken within about 10-km of the mooring. The current speeds were respectively about 20 cm s^{-1} and 10 cm s^{-1} near the beginning and end of the records. The predicted bottom-layer thicknesses (vertical scales)

would be respectively 27 m and 13 m. CTD temperature data from 2009 and 2010 are shown in Figure 40; the profiles are replotted on the right versus height off the bottom. One of the casts may have a bottom mixed-layer thickness of about 100 m (CTD F01 in 2010). All together the CTD observations do not indicate that the moored instruments were measurably affected by bottom boundary layer effects.

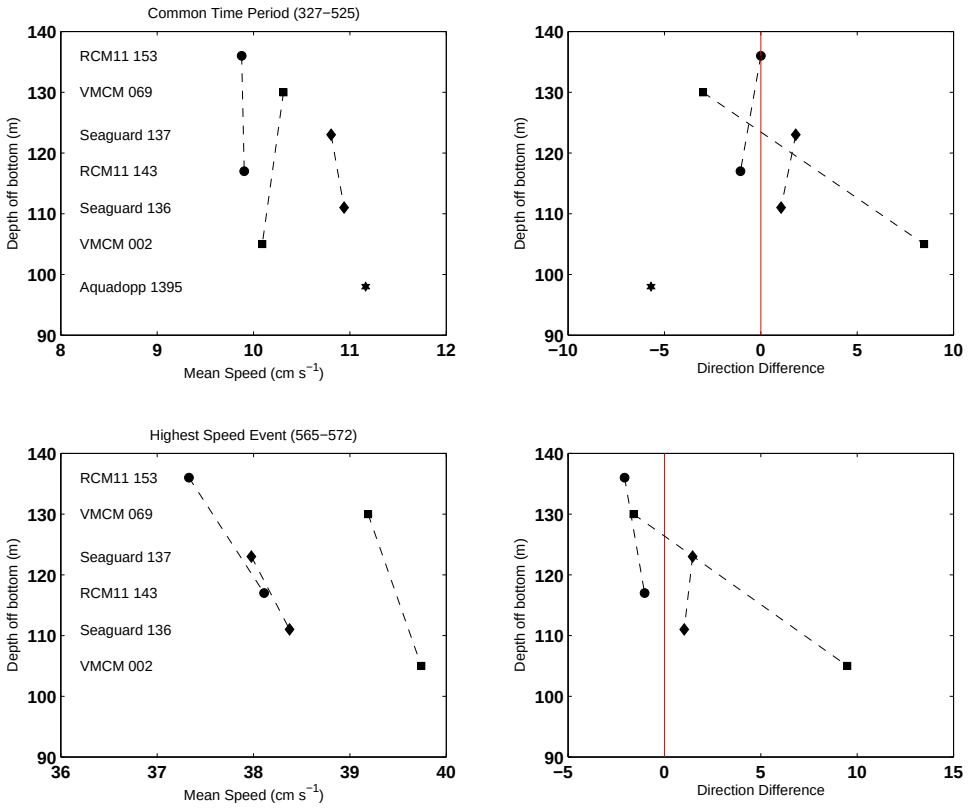

Figure 39: Mean vector-averaged speeds and direction difference from the median are shown for two time periods (top): the common period (days 327–525) and (bottom): highest speed event (days 565–572). 30-minute intervals in which any VMCM rotor stalled were not used in the calculations. Data from the same current meter model are connected by the dashed lines. In the common time period, speed differences associate with model and not with height above the bottom. In the highest speed event the three models show higher speeds at the lower current meter, which suggests about 1.3% bottom intensification in the approximately 30 m span of depths. The current directions do not turn significantly with height off the bottom.

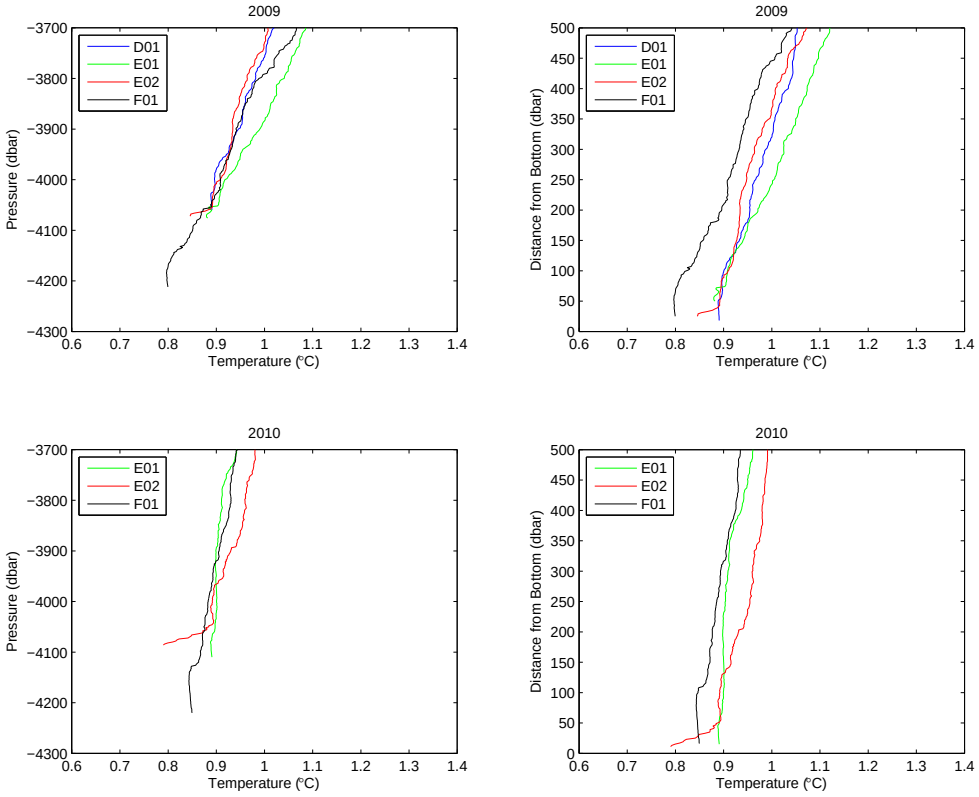

Figure 40: Left panels: CTD temperature as a function of pressure and right panels are CTD temperature replotted versus distance from bottom for 2009 and 2010. See Figure 2 for locations of the CTD casts.

References

Bishop, S. P., D. R. Watts, J.-H. Park, and N. G. Hogg (2011), Evidence of bottom-trapped currents in the Kuroshio Extension region, *J. Phys. Oceanogr.*, *42*(2), 321–328.

Chereskin, T. K., K. A. Donohue, D. R. Watts, K. L. Tracey, Y. Firing, and A. L. Cutting (2009), Strong bottom currents and cyclonesis in Drake Passage, *Geophys. Res. Lett.*, *36*(L23602), doi:10.1029/2009GL040940.

Dickey, T. D., A. J. Plueddemann, and R. A. Weller (1998), Current and water property measurements in the coastal ocean. The Sea – Ideas and Observations on Progress in the Study of the Seas, in *The Global Coastal Ocean*, vol. 10, edited by K. H. Brink and A. R. Robinson, pp. 367–398, John Wiley and Sons.

Drozdowski, A., and B. J. W. Greenan (2012), An intercomparison of acoustic current meters deployed on the Scotian Shelf, *Canadian Technical Report of Hydrography and Ocean Sciences (in press)*, Bedford Institute of Oceanography.

Drozdowski, A., B. J. W. Greenan, M. D. Scotney, J. W. Loder, and Y. Geshelin (2010), An intercomparison of acoustic current meters deployed on the Scotian Shelf, *Canadian Technical Report of Hydrography and Ocean Sciences 264*, Bedford Institute of Oceanography.

Gilboy, T. P., T. D. Dickey, D. E. Sigurdson, X. Yu, and D. Manov (2000), An intercomparison of current measurements using a vector measuring current meter, an acoustic doppler current profiler, and a recently developed acoustic current meter, *J. Atmos Oceanic Technol.*, *17*, 561–574.

Hogg, N. G., and D. E. Frye (2007), Performance of a new generation of acoustic current meters, *J. Phys. Oceanogr.*, *37*(2), 148–161, doi:10.1175/JPO303.1.

Victoria, I. (2011), Measuring currents in demanding environments with a Seaguard®RCM, in *Proceedings of the IEEE/OES/CWTM Tenth Working Conference on Current Measurement Technology*, pp. 237–245, Monterey, California.

Weller, R. A., and R. E. Davis (1980), A vector measuring current meter, *Deep Sea Research Part A. Oceanographic Research Papers*, *27*(7), 565 – 566, IN1–IN2, 567–581, doi:DOI: 10.1016/0198-0149(80)90041-2.